1969

Spread in flat rolling

Richard D. Way
Lehigh University

SPREAD IN FLAT ROLLING

By

R. D. Way

A THESIS

Presented to the Graduate Committee

of Lehigh University

in Candidacy for the Degree of

Master of Science

in

Mechanical Engineering

Lehigh University

1969

CERTIFICATE OF APPROVAL

This thesis is accepted and approved in partial fulfillment of the requirements for the degree of Master of Science.

May 9 1969
(Date)

Betzalel Avitzur
Professor in Charge

Ferdinand P. Beer
Chairman of the Department

ACKNOWLEDGEMENTS

The author is indebted to Dr. B. Avitzur, Professor of Metallurgy and Materials Science, for suggesting the subject of this thesis. Dr. Avitzur's guidance and suggestions throughout the course of this work are greatly appreciated. Also, thanks to Dr. S. Iscovici for helpful comments on handling of the mathematics.

Thanks are due to the Bethlehem Steel Corporation, Research Department, for computer, library, and stenographic services provided the author. In addition, the author extends his gratitude to Bethlehem Steel for making possible the pursuit of his Master's Degree through its Educational Assistance Program.

Finally, special thanks go to the author's family for their indulgence and understanding during the long, and often odd, hours of work and study.

TABLE OF CONTENTS

TABLE OF CONTENTS
(Continued)

LIST OF FIGURES AND TABLES

ABSTRACT

A velocity field was derived for a flat workpiece undergoing plastic deformation between cylindrical rolls in a rolling mill. Using the velocity field, an expression was written for the total power input required for the rolling process in terms of the process parameters: roll diameter, thickness reduction, workpiece geometry, surface friction, and spread. The Upper Bound Theorem was applied to the power expression to establish an upper limit on it. This limit was minimized with respect to spread to determine the value of spread requiring the least amount of input power. This value was taken as the spread that will occur in the actual rolling process. Due to the bulky nature of the power limit expression the minimization was handled with a digital computer.

The analytical spread model was used to predict the effect of rolling process conditions on the degree of spreading. Comparisons were made between predicted spread and experimental spread data published by several investigators. The effects of roll size, reduction, workpiece geometry, and friction are correctly predicted by the analytical spread model. In most cases, however, the degree of spreading is underestimated by the model in comparison with experimental data. This is attributed to the simplifying assumptions made in the analysis. It is recommended that this work be extended without the restrictions of these assumptions.

INTRODUCTION

Background

In the rolling of metals, Figure 1, the workpiece is squeezed between parallel rotating rolls and becomes thinner, longer and wider. Often the workpiece is given a series of passes through a single rolling mill to accomplish the desired dimensional changes. In order to finish the workpiece at the proper size, it is necessary to know how the dimensions will change with each succeeding pass through the rolling mill and to adjust the roll gap accordingly.

Investigators who have directed their attention to the width change, or spread, of the workpiece have all used the empirical approach of finding a formula to fit experimental data. Siebel[1] and Sedlaczek[2] were among the early investigators of spread in rolling. Wusatowski[4-8] has been the most active writer in this field with his work covering the period 1947 to 1967. Ekelund,[10] Hill,[10] and Sparling[9] have also contributed important work on the prediction of spread using empirical formulas.

Siebel derived his empirical spread formula from data published by Falk.[1] The formula is:

$$b_2 - b_1 = c_1(h_1 - h_2)\frac{\sqrt{R^2-\left(R-\frac{h_1+h_2}{2}\right)^2}}{h_1}$$

where: $0.3 \leq c_1 \leq 0.4$

Later experiments by A. Spenle and O. Emicke - E. Pachaly[2] proved Siebel's simple formula to be inaccurate for rolling conditions different from those used by Falk.

Sedlaczek's formula predicted spread more accurately than Siebel's when it was checked experimentally by these investigators. His formula is:

$$b_2 - b_1 = \frac{b_1\sqrt{Rb_1}\,(h_1-h_2)}{3(b_1^2+h_1h_2)}$$

The improvement in accuracy over Siebel's formula is due mainly to the inclusion of workpiece starting width, b_1, as a variable.

Ekelund's empirically derived spread formula went a step further by including roll/workpiece friction as a variable affecting spread:

$$b_2^2 - b_1^2 = \left[8\Delta h - 4\ell n\left(\frac{b_2}{b_1}\right)(h_1+h_2)\right](R\Delta h)^{1/2}\left[\frac{1.6\mu(R\Delta h)^{1/2} - 1.2\Delta h}{h_1+h_2}\right]$$

where: μ = coefficient of coulomb friction

This formula is very difficult to use because it is an implicit relationship for the spread, b_2-b_1. McCrum[11] carried out critical tests to determine the accuracy of three spread formulas, including Ekelund's, and concluded that Ekelund's was least accurate of the three.

The other two spread formulas checked by McCrum were those of Wusatowski and Hill. Wusatowski's formula is:

$$\frac{b_2}{b_1} = a'b'c'd'\left(\frac{h_1}{h_2}\right)^p$$

where: a' = steel composition factor

b' = rolling temperature factor

c' = rolling speed factor

d' = roll material factor

$$p = 10^{-1.269\left(\frac{b_1}{h_1}\right)\left(\frac{h_1}{D}\right)^{0.556}}$$

(The constants 1.269 and 0.556 were later changed to 3.954 and 0.9676).

Although a friction coefficient does not appear in Wusatowski's formula, the above four factors all help to account for frictional conditions. This formula has been checked against experimental data by Wusatowski and other investigators. Although it does not describe what physically happens in the rolling process, it has been found to be reasonably accurate and is generally used as the standard by which to judge new work in this field.

Hill suggested the following formula:

$$\log\left(\frac{b_2}{b_1}\right) = 0.5\, e^{-\frac{1}{2} b_1/\sqrt{D\Delta h}} \cdot \log\left(\frac{h_1}{h_2}\right)$$

The factor 1/2 in the exponent is arbitrary and must be modified to fit experimental data. The effect of roll/workpiece friction is not included in Hill's formula.

Sparling also investigated the accuracy of Wusatowski's and Hill's formulas by conducting rolling experiments on a laboratory and an industrial rolling mill. He found that Wusatowski's formula gave better results than Hill's. In addition, Sparling was able to develop his own spread formula which gave even better results than Wusatowski's. Sparling's formula is:

$$\frac{b_2}{b_1} = \left(\frac{h_1}{h_2}\right)^{0.981 e^{-0.6735\left[2.395\, b_1^{0.9}\left(\frac{1}{R}\right)^{0.55}\left(\frac{1}{h_1}\right)^{0.1}\left(\frac{1}{\Delta h}\right)^{0.25}\right] abfgj}}$$

where: a = roll surface condition factor

b = workpiece surface condition factor

f = workpiece composition factor

g = temperature factor

j = mean strain rate

In 35 tests on the two rolling mills used by Sparling, the spread predicted by his formula was within 10% of the measured spread about 90% of the time. The corresponding figure for Wusatowski's formula was about 50% of the time and for Hill's formula about 9% of the time.

Analytical Approach

Unlike the empirical work done by the previous investigators, this present work will utilize an analytical approach to solve the spread problem. The Upper Bound Theorem, formulated by Prager and Hodge,[12] will be used to derive a model of workpiece spread in flat rolling that has some physical meaning.

A process takes place in nature in the most economical manner as far as energy is concerned. The path of least resistance is automatically utilized. To make use of this principle, a velocity field was derived and used to write an expression, in terms of the process variables, for the total power required to deform a flat workpiece between cylindrical rolls. The spread, b_2/b_1, was treated as a variable and the power expression was minimized with respect to the spread. The unique value of b_2/b_1 that resulted in the lowest required power input to the process was taken as the solution to the problem.

Assumptions

The following simplifying assumptions were made at the outset:

1. The workpiece has a rectangular cross-section both before and after deformation. There is no warping or bulging of the sides.
2. The workpiece material obeys Mises' stress-strain rate law.* There is no strain hardening.
3. The mill rolls are rigid and do not deform from their unloaded condition.

---

*For the ramification of this assumption, see Reference 12, p 50.

4. Friction obeys the law $\tau = m \frac{\sigma_o}{\sqrt{3}}$ where τ is the frictional shear stress, m is a friction factor assumed to remain constant throughout the roll contact zone for given rolling conditions, and $\frac{\sigma_o}{\sqrt{3}}$ is the value of k for Mises' yield criteria.[12] Friction factor m is influenced by surface conditions, but not by pressure or velocity. The condition $0 \leq m \leq 1$ must hold. $m = 0$ implies frictionless conditions while $m = 1.0$ implies sticking of the workpiece to the rolls.

In addition to these assumptions, it was later found necessary to restrict the value of the no-slip angle, α_n, to $\alpha_n = 0$ in order to keep the analysis within the scope of this work.* The effect of this and the other assumptions on the spread predicted by the analysis will be discussed later.

---

*The no-slip angle locates the point (Figure 2) where roll and workpiece have the same velocity. Between the no-slip point and the entry plane (S_1 in Figure 2) the rolls are moving faster than the workpiece. Between the no-slip point and the exit plane (S_2 in Figure 2) the rolls are moving slower than the workpiece.

UPPER BOUND ANALYSIS OF SPREAD

In the flat rolling process, the workpiece is introduced between a pair of parallel rolls, Figure 1, which compress it and make it thinner, longer and wider. Figure 4 shows the portion of the workpiece undergoing plastic deformation in the contact zone between the rolls. Power is expended to deform the workpiece from entering conditions (h_1, b_1, V_1) to exit conditions (h_2, b_2, V_2). Density and volume of the workpiece remain essentially unchanged during the plastic deformation. The total rolling power can be divided into four distinct parts: (a) internal power of deformation ($\dot{W}_I$), (b) shear-loss power at surface S_1 in Figure 4 ($\dot{W}_{S_1}$), (c) shear-loss power at surface S_2 in Figure 4 ($\dot{W}_{S_2}$), and (d) friction-loss power at surfaces S_3 in Figure 4 ($\dot{W}_F$).

$\dot{W}_I$ is the power required to deform the workpiece from (h_1, b_1, V_1) to (h_2, b_2, V_2) in the absence of any losses. $\dot{W}_{S_1}$ and $\dot{W}_{S_2}$ arise because power is lost in changing the direction of the workpiece velocity vector at surfaces S_1 and S_2 (surfaces of velocity discontinuity). $\dot{W}_F$ accounts for the power lost in overcoming surface friction between the rolls and workpiece at surfaces S_3. These are also treated as surfaces of velocity discontinuity.

Upper Bound Theorem

The spread problem is solved through Upper Bound Analysis. The Upper Bound Theorem was formulated by Prager and Hodge.[13] Avitzur[14] stated it as follows:

> "Among all kinematically admissible strain rate fields, the actual one minimizes the expression "

$$J^* = \frac{2}{\sqrt{3}} \sigma_0 \int_V \sqrt{\tfrac{1}{2} \dot{\varepsilon}_{ij} \dot{\varepsilon}_{ij}}\, dV + \int_{S\Gamma} \tau |\Delta V|\, ds - \int_{St} T_i V_i\, ds \qquad (5.27)$$

A strain rate field derived from a kinematically admissible velocity field is kinematically admissible.

J^* is the actual externally supplied power and can never be greater than that computed with the above equation. The first term is the internal power of deformation over the workpiece volume, and is the power required to deform the workpiece in the absence of any losses. The second term is the power "loss" due to shear at surfaces of velocity discontinuity. Such surfaces are the roll/workpiece contact surfaces (S_3 in Figure 2) and the internal shear surfaces bounding the deformation zone in the workpiece (S_1 and S_2 in Figure 2). The third term is power supplied by external body tractions such as front and back tensions in rolling. These tractions are not considered in this analysis.

The following procedure was used to derive a model of spread in flat rolling.

1. A kinematically admissible velocity field was derived for the workpiece deformation zone.
2. The strain rates in the principal directions were calculated from the velocity field, and Equation (5.27) was written in terms of the rolling variables. The spread was treated as a variable.
3. The actual J* cannot be larger than that calculated by Equation (5.27). Equation (5.27) was minimized with respect to spread. The unique value of spread that minimized Equation (5.27) was taken as the spread that actually occurs.

A more rigorous approach would be to confine J* between an Upper and Lower Bound. By minimizing the Upper Bound and maximizing The Lower Bound, the solution for spread would be more accurately determined. However, Lower Bound analysis is not as well developed as Upper Bound analysis at this time and is beyond the scope of this work.

Velocity Field Derivation

Constant workpiece volume during rolling requires:

$$V_y bh = V_2 b_2 h_2 = V_R \cos\alpha_m b_m h_m = V_1 b_1 h_1 \qquad (1)$$

From Figure 2, the following geometric relationship is observed:

$$y = L - R\sin\alpha$$

Rearranging:

$$\sin\alpha = \frac{L-Y}{R}$$

Taking the derivative with respect to y:

$$\cos\alpha \frac{d\alpha}{dY} = -\frac{1}{R}$$

$$\frac{d\alpha}{dY} = -\frac{1}{R\cos\alpha} \qquad (2a)$$

Another geometric relationship from Figure 2 is:

$$R\cos\alpha_1 = R - \frac{h_1 - h_2}{2}$$

$$\cos\alpha_1 = 1 - \frac{h_1 - h_2}{2R}$$

Using the small angle approximation $\cos\alpha_1 \cong 1 - \frac{\alpha_1^2}{2}$:

$$1 - \frac{\alpha_1^2}{2} = 1 - \frac{h_1 - h_2}{2R}$$

$$\alpha_1 = \sqrt{\frac{h_2}{R}\left(\frac{h_1}{h_2} - 1\right)} \qquad (2b)$$

The workpiece thickness at any point between the rolls is (Figure 2):

$$h = h_2 + 2(R - R\cos\alpha)$$

Applying the small angle approximation for $\cos\alpha$:

$$h = h_2 + R\alpha^2 \qquad (3a)$$

Similarly:

$$h_m = h_2 + R\alpha_m^2 \quad \text{(Thickness at no-slip angle)} \qquad (3b)$$

$$h_1 = h_2 + R\alpha_1^2 \quad \text{(Thickness at entry plane)} \qquad (3c)$$

The workpiece width at any point between the rolls is (Figure 1):

$$b = b_2 + \frac{\alpha}{\alpha_1}(b_1 - b_2) \tag{4a}$$

Similarly:

$$b_m = b_2 + \frac{\alpha_m}{\alpha_1}(b_1 - b_2) \tag{4b}$$

From the constant volume relationship, Equation (1):

$$V_y = V_R\left(\frac{b_m}{b}\right)\left(\frac{h_m}{h}\right)\cos\alpha_m$$

Applying Equations (3) and (4):

$$V_y = V_R \frac{\left[b_2 + \frac{\alpha_m}{\alpha_1}(b_1 - b_2)\right](h_2 + R\alpha_m^2)}{\left[b_2 + \frac{\alpha}{\alpha_1}(b_1 - b_2)\right](h_2 + R\alpha^2)}\cos\alpha_m \tag{5a}$$

Rearranging:

$$V_y = V_R \frac{\left[\frac{b_2}{b_1} + \frac{\alpha_m}{\alpha_1}\left(1 - \frac{b_2}{b_1}\right)\right]\left(\frac{h_2}{R} + \alpha_m^2\right)}{\left[\frac{b_2}{b_1} + \frac{\alpha}{\alpha_1}\left(1 - \frac{b_2}{b_1}\right)\right]\left(\frac{h_2}{R} + \alpha^2\right)}\cos\alpha_m \tag{5b}$$

The workpiece width at any point between the rolls is given by Equation (4a). Taking the time derivative of this equation:

$$\frac{db}{dt} = 0 + \frac{b_1 - b_2}{\alpha_1} \cdot \frac{d\alpha}{dt} = \frac{b_1 - b_2}{\alpha_1} \cdot \frac{d\alpha}{dY} \cdot \frac{dY}{dt}$$

Substituting for $\frac{d\alpha}{dY}$ from Equation (2):

$$\frac{db}{dt} = \frac{b_1 - b_2}{\alpha_1}\left(-\frac{1}{R\cos\alpha}\right)V_y$$

V_X is assumed to be linear in X. The end conditions are:

$$V_x\Big|_{x=0} = 0$$

$$V_x\Big|_{x=\frac{b}{2}} = \frac{1}{2}\cdot\frac{db}{dt}$$

These conditions are satisfied by the following equation:

$$V_x = \frac{b_2-b_1}{\alpha_1}\cdot\frac{V_Y}{R\cos\alpha}\cdot\frac{X}{b}$$

Substituting for b from Equation (4a):

$$V_x = \frac{\left(\frac{b_2}{b_1}-1\right)X\,V_Y}{R\alpha_1\cos\alpha\left[\frac{b_2}{b_1}+\frac{\alpha}{\alpha_1}\left(1-\frac{b_2}{b_1}\right)\right]} \qquad (6)$$

At the roll surface (i.e., Z = h/2) in Figure 3:

$$\tan\alpha = -\frac{V_Z}{V_Y}$$

V_Z is assumed to be linear in Z. The end conditions are:

$$V_z\Big|_{z=0} = 0$$

$$V_z\Big|_{z=\frac{h}{2}} = -V_Y\tan\alpha$$

These conditions are met by the following equation:

$$V_z = -\frac{V_Y\tan\alpha}{\frac{h}{2}}\cdot Z$$

Substituting for h from Equation (3a):

$$V_z = -\frac{2V_Y \tan\alpha}{h_2 + R\alpha^2} Z \tag{7}$$

The velocity field is completely defined through Equations (5b), (6), and (7). The condition of incompressibility,

$$\dot{\varepsilon}_{xx} + \dot{\varepsilon}_{yy} + \dot{\varepsilon}_{zz} = 0$$

Where:

$$\dot{\varepsilon}_{xx} = \frac{\partial V_x}{\partial X}$$

$$\dot{\varepsilon}_{yy} = \frac{\partial V_Y}{\partial Y}$$

$$\dot{\varepsilon}_{zz} = \frac{\partial V_z}{\partial Z}$$

is satisfied by the velocity field.

Internal Power of Deformation

Avitzur[15] has shown that the work per unit volume required to deform a workpiece in the absence of losses is:

$$\omega_i = \frac{2}{\sqrt{3}} \sigma_0 \sqrt{\frac{1}{2}\left(\varepsilon_I^2 + \varepsilon_{II}^2 + \varepsilon_{III}^2\right)} \tag{8}$$

where $\varepsilon_I, \varepsilon_{II}, \varepsilon_{III}$ are the true strains in the principal directions; i.e., the X, Y, and-Z directions for this case.

$$\varepsilon_I = \varepsilon_{xx} = \ln \frac{b_2}{b_1} \tag{9a}$$

$$\varepsilon_{II} = \varepsilon_{yy} = \ln \frac{l_2}{l_1} \tag{9b}$$

$$\varepsilon_{III} = \varepsilon_{zz} = \ln \frac{h_2}{h_1} \tag{9c}$$

Incompressibility also dictates:

$$\varepsilon_{xx} + \varepsilon_{yy} + \varepsilon_{zz} = 0$$

Therefore:

$$\varepsilon_{yy} = -(\varepsilon_{xx} + \varepsilon_{zz})$$

$$\varepsilon_{yy} = -\left(\ln \frac{b_2}{b_1} + \ln \frac{h_2}{h_1}\right) \tag{10}$$

Substituting Equations (9a), (9c), and (10) into Equation (8) gives:

$$\omega_i = \frac{2}{\sqrt{3}} \sigma_0 \ln\left(\frac{b_2}{b_1}\right) \sqrt{1 + \frac{\ln\left(\frac{h_2}{h_1}\right)}{\ln\left(\frac{b_2}{b_1}\right)} + \left[\frac{\ln\left(\frac{h_2}{h_1}\right)}{\ln\left(\frac{b_2}{b_1}\right)}\right]^2} \tag{11}$$

The total internal power of deformation is obtained from the work per unit volume by the relationship:

$$\dot{W}_I = \omega_i \dot{V} \qquad (12)$$

Where: $\dot{V}$ = volume rate = $b_m h_m V_R \cos\alpha_m$.

Substituting the above expression into Equation (12):

$$\dot{W}_I = \frac{2}{\sqrt{3}} \sigma_o \ln\left(\frac{b_2}{b_1}\right) \sqrt{1 + \frac{\ln\left(\frac{h_2}{h_1}\right)}{\ln\left(\frac{b_2}{b_1}\right)} + \left[\frac{\ln\left(\frac{h_2}{h_1}\right)}{\ln\left(\frac{b_2}{b_1}\right)}\right]^2} \cdot$$

$$b_m h_m V_R \cos\alpha_m \qquad (13a)$$

Substituting Equations (3b) and (4b) into Equation (13a) and rearranging:

$$\frac{\dot{W}_I}{\frac{\sigma_o V_R R^2}{\sqrt{3}}} = 2\left(\frac{b_1}{R}\right)\left[\ln\left(\frac{b_2}{b_1}\right)\right]\left[\frac{h_2}{R} + \alpha_m^2\right]\left[\frac{b_2}{b_1} + \frac{\alpha_m}{\alpha_1}\left(1 - \frac{b_2}{b_1}\right)\right] \cdot$$

$$\sqrt{1 - \frac{\ln\left(\frac{h_1}{h_2}\right)}{\ln\left(\frac{b_2}{b_1}\right)} + \left[\frac{\ln\left(\frac{h_1}{h_2}\right)}{\ln\left(\frac{b_2}{b_1}\right)}\right]^2} \cos\alpha_m \qquad (13b)$$

$\frac{\dot{W}_I}{\frac{\sigma_o V_R R^2}{\sqrt{3}}}$ is a convenient non-dimensional form of the internal power of deformation.

Shear Loss Power at Entry Plane

At surface S_1 in Figure 2, there is redundant power expended due to the existence of a velocity discontinuity. Avitzur[16] has shown that the power required to overcome a velocity discontinuity is:

$$\dot{W} = \int_S \tau \Delta V \, ds = \int_S \frac{m\sigma_o}{\sqrt{3}} \Delta V \, ds \tag{14a}$$

Where τ is the shear stress, S denotes the surface of velocity discontinuity, and m is a shear factor of value unity for the workpiece shearing on itself. For surface S_1:

$$\dot{W}_{S1} = \frac{\sigma_o}{\sqrt{3}} \int_{S1} \Delta V_1 \, dS_1 \tag{14b}$$

The velocity is discontinuous in more than one direction, and ΔV_1 is the resultant velocity discontinuity existing at any point on S_1.

$$\Delta V_1^2 = \Delta V_x^2 + \Delta V_y^2 + \Delta V_z^2 \tag{15}$$

The individual velocity discontinuities are:

$$\Delta V_x = V_x\big|_{\alpha=\alpha_1} - 0 \tag{16a}$$

$$\Delta V_y = V_y\big|_{\alpha=\alpha_1} - V_1 \tag{16b}$$

$$\Delta V_z = V_z\big|_{\alpha=\alpha_1} - 0 \tag{16c}$$

It follows from Equation (1) that:

$$V_y\big|_{\alpha=\alpha_1} = \frac{V_R b_m h_m \cos\alpha_m}{b_1 h_1} = V_1 \tag{17a}$$

Substituting Equation (17a) into Equation (6):

$$V_x\Big|_{\alpha=\alpha_1} = \frac{V_R\left(\frac{b_2}{b_1}-1\right) b_m h_m \cos\alpha_m}{R\alpha_1 b_1 h_1 \cos\alpha_1} X \tag{17b}$$

Substituting Equation (17a) into Equation (7):

$$V_z\Big|_{\alpha=\alpha_1} = \frac{-2V_R \tan\alpha_1 b_m h_m \cos\alpha_m}{b_1 h_1^2} Z \tag{17c}$$

Combining Equations (15), (16), and (17) yields the required velocity discontinuity at S_1:

$$\Delta V_1 = \frac{V_R \cos\alpha_m}{R} \sqrt{\frac{\left(\frac{b_2}{b_1}-1\right)^2 b_m^2 h_m^2 X^2}{\alpha_1^2 b_1^2 h_1^2 \cos^2\alpha_1} + \frac{4R^2 \tan^2\alpha_1 b_m^2 h_m^2 Z^2}{b_1^2 h_1^4}} \tag{18}$$

This expression has the form: $\frac{V_R \cos\alpha_m}{R}\sqrt{a_1 X^2 + c_1}$

where a_1 and c_1 are constants with respect to X.

The shear loss power at surface S_1 thus becomes:

$$\dot{W}_{s_1} = \frac{4\sigma_0 V_R \cos\alpha_m}{R\sqrt{3}} \int_{Z=0}^{Z=\frac{h_1}{2}} \int_{X=0}^{X=\frac{b_1}{2}} \sqrt{a_1 X^2 + c_1}\, dx\, dz \tag{19}$$

The integration is made for X by using integral No. 112 in Burington.[17] The integration for Z requires (a) integration by parts, (b) integral No. 120 in Burington, and (c) use of l'Hôpital's Rule for indeterminate forms. The integration is carried out in detail in Appendix II.

The shear loss power at S_1 then becomes:

$$\frac{\dot{W}_{S_1}}{\frac{\sigma_0 V_R R^2}{\sqrt{3}}} = \cos\alpha_m \left[\frac{b_2}{b_1} + \frac{\alpha_m}{\alpha_1}\left(1 - \frac{b_2}{b_1}\right)\right]\left[\frac{h_2}{R} + \alpha_m^2\right] \cdot$$

$$\left\langle \frac{\left(\frac{b_1}{R}\right)^2\left(\frac{b_2}{b_1} - 1\right)}{6\sqrt{\frac{h_2}{R}\left(\frac{h_1}{h_2} - 1\right)}\,\cos\sqrt{\frac{h_2}{R}\left(\frac{h_1}{h_2} - 1\right)}} \right.$$

$$\sqrt{1 + \frac{4\left(\frac{h_2}{R}\right)\left(\frac{h_1}{h_2} - 1\right)\sin^2\sqrt{\frac{h_2}{R}\left(\frac{h_1}{h_2} - 1\right)}}{\left(\frac{b_2}{b_1} - 1\right)^2\left(\frac{b_1}{R}\right)^2}} \; +$$

$$\left. \frac{\left(\frac{b_2}{b_1} - 1\right)^2\left(\frac{b_1}{R}\right)^3}{24\left(\frac{h_2}{R}\right)\left(\frac{h_1}{h_2} - 1\right)\sin\sqrt{\frac{h_2}{R}\left(\frac{h_1}{h_2} - 1\right)}\,\cos\sqrt{\frac{h_2}{R}\left(\frac{h_1}{h_2} - 1\right)}} \right\rangle \cdot$$

$$\ln\left[\frac{2\sqrt{\frac{h_2}{R}\left(\frac{h_1}{h_2}-1\right)}\sin\sqrt{\frac{h_2}{R}\left(\frac{h_1}{h_2}-1\right)}}{\left(\frac{D_2}{D_1}-1\right)\left(\frac{D_1}{R}\right)}+\right.$$

$$\left.\sqrt{1+\frac{4\left(\frac{h_2}{R}\right)\left(\frac{h_1}{h_2}-1\right)\sin^2\sqrt{\frac{h_2}{R}\left(\frac{h_1}{h_2}-1\right)}}{\left(\frac{D_2}{D_1}-1\right)^2\left(\frac{D_1}{R}\right)^2}}\right]+$$

$$\frac{\sqrt{\left(\frac{h_2}{R}\right)\left(\frac{h_1}{h_2}-1\right)}\tan^2\sqrt{\frac{h_2}{R}\left(\frac{h_1}{h_2}-1\right)}\cos\sqrt{\frac{h_2}{R}\left(\frac{h_1}{h_2}-1\right)}}{3\left(\frac{D_2}{D_1}-1\right)}.$$

$$\ln\left\{\frac{\left(\frac{D_2}{D_1}-1\right)\left(\frac{D_1}{R}\right)}{2\sqrt{\frac{h_2}{R}\left(\frac{h_1}{h_2}-1\right)}\sin\sqrt{\frac{h_2}{R}\left(\frac{h_1}{h_2}-1\right)}}\cdot\right.$$

$$\left.\left[1+\sqrt{1+\frac{4\left(\frac{h_2}{R}\right)\left(\frac{h_1}{h_2}-1\right)\sin^2\sqrt{\frac{h_2}{R}\left(\frac{h_1}{h_2}-1\right)}}{\left(\frac{D_2}{D_1}-1\right)^2\left(\frac{D_1}{R}\right)^2}}\right]\right\}\rangle \quad (20)$$

$\frac{\dot{W}_{S1}}{\frac{\sigma_0 V_R R^2}{\sqrt{3}}}$ is a convenient non-dimensional form of the shear loss power at the entry plane.

Shear Loss Power at Exit Plane

At surface S_2 in Figure 2, redundant power is expended due to the velocity discontinuity in the width direction. The power required to overcome this velocity discontinuity is:

$$\dot{W}_{S_2} = \frac{\sigma_0}{\sqrt{3}} \int_{S_2} \Delta V_2 \, dS_2 \tag{21}$$

Proceeding as in the case of $\dot{W}_{S_1}$:

$$\Delta V_2^2 = \Delta V_x^2 + \Delta V_y^2 + \Delta V_z^2 \tag{22}$$

Where:

$$\Delta V_x = V_x\big|_{\alpha=0} - 0 \tag{23a}$$

$$\Delta V_y = V_y\big|_{\alpha=0} - V_2 \tag{23b}$$

$$\Delta V_z = V_z\big|_{\alpha=0} - 0 \tag{23c}$$

It follows from Equation (1) that:

$$V_y\big|_{\alpha=0} = \frac{V_2 b_2 h_2}{b_2 h_2} = V_2 \tag{24a}$$

Substituting Equation (24a) into Equation (6):

$$V_x\Big|_{\alpha=0} = \frac{V_2\left(\frac{b_2}{b_1}-1\right)}{R\alpha_1\left(\frac{b_2}{b_1}\right)} \tag{24b}$$

Substituting Equation (24a) into Equation (7):

$$V_z\Big|_{\alpha=0} = \frac{-2\,V_2(0)}{h_2+R(0)}\,z = 0 \tag{24c}$$

Combining Equations (22), (23), and (24) yields the required velocity discontinuity at S_2:

$$\Delta V_2 = \frac{V_2\left(\frac{b_2}{b_1}-1\right)}{R\alpha_1\left(\frac{b_2}{b_1}\right)}\,X \tag{25}$$

The shear loss power at surface S_2 thus becomes:

$$\dot{W}_{S_2} = \frac{4\sigma_0 V_2\left(\frac{b_2}{b_1}-1\right)}{\sqrt{3}\,R\alpha_1\left(\frac{b_2}{b_1}\right)} \int_{z=0}^{z=\frac{h_2}{2}} \int_{x=0}^{x=\frac{b_2}{2}} X\,dx\,dz \tag{26}$$

Performing the integration with respect to X:

$$\dot{W}_{S_2} = \frac{4\sigma_0 V_2\left(\frac{b_2}{b_1}-1\right)}{\sqrt{3}\,R\alpha_1\left(\frac{b_2}{b_1}\right)} \int_{z=0}^{z=\frac{h_2}{2}} \left(\frac{X^2}{2}\Big|_0^{\frac{b_2}{2}}\right) dz$$

Simplifying:

$$\dot{W}_{S_2} = \frac{\sigma_0 V_2 \left(\frac{b_2}{b_1} - 1\right) b_2^2}{2\sqrt{3}\, R \alpha_1 \left(\frac{b_2}{b_1}\right)} \int_{z=0}^{z=\frac{h_2}{2}} dz \qquad (27)$$

Performing the integration with respect to Z:

$$\dot{W}_{S_2} = \frac{\sigma_0 V_2 b_2^2 \left(\frac{b_2}{b_1} - 1\right)}{2\sqrt{3}\, R \alpha_1 \left(\frac{b_2}{b_1}\right)} \left(\frac{h_2}{2}\right) \qquad (28)$$

Rearranging, and using Equation (1):

$$\dot{W}_{S_2} = \frac{\sigma_0 \left(\frac{b_2}{b_1} - 1\right)\left(\frac{b_1}{R}\right) V_R b_m h_m \cos\alpha_m}{4\sqrt{3}\, \alpha_1}$$

Substituting Equations (3b) and (4b) and rearranging:

$$\frac{\dot{W}_{S_2}}{\frac{\sigma_0 V_R R^2}{\sqrt{3}}} = \frac{1}{4\alpha_1}\left(\frac{b_2}{b_1} - 1\right)\left[\frac{b_2}{b_1} + \frac{\alpha_m}{\alpha_1}\left(1 - \frac{b_2}{b_1}\right)\right]\left[\frac{h_2}{R} + \alpha_m^2\right] \cdot$$

$$\left(\frac{b_1}{R}\right)^2 \cos\alpha_m \qquad (29)$$

$\frac{\dot{W}_{S_2}}{\frac{\sigma_0 V_R R^2}{\sqrt{3}}}$ is a convenient non-dimensional form of the shear loss power at the exit plane.

Friction Loss Power at Roll Surface

At the surfaces of contact between workpiece and rolls (S_3 in Figure 4) there is power lost in overcoming friction. This power is expressed using Equation (14a):

$$\dot{W}_F = 2\int_{S_3} \frac{m\sigma_o}{\sqrt{3}} \Delta V_3 \, dS_3 \tag{30}$$

Where: m = shear factor due to friction

ΔV_3 = resultant velocity discontinuity on S_3

dS_3 = incremental area on surface S_3

Using geometrical symmetry and Figure 4, the expression becomes:

$$\dot{W}_F = \frac{4m\sigma_o}{\sqrt{3}} \int_{\alpha=0}^{\alpha=\alpha_1} \int_{x=0}^{x=\frac{b}{2}} \Delta V_3 \, dx \, R \, d\alpha \tag{31}$$

As shown in Figure 3, the velocity of the workpiece at surface S_3 is made up of a component tangent to the roll surface and normal to the roll axis (V_{TR}), and a component tangent to the roll surface and parallel to the roll axis (V_X).

Combining Equations (5b) and (6):

$$V_X = \frac{\left(\frac{b_2}{b_1}-1\right) V_R \left[\frac{b_2}{b_1} + \frac{\alpha_M}{\alpha_1}\left(1-\frac{b_2}{b_1}\right)\right]\left(\frac{h_2}{R}+\alpha_M^2\right) X \cos\alpha_M}{R\alpha_1 \cos\alpha \left[\frac{b_2}{b_1} + \frac{\alpha}{\alpha_1}\left(1-\frac{b_2}{b_1}\right)\right]^2 \left(\frac{h_2}{R}+\alpha^2\right)} \tag{32}$$

From Figure (3):

$$V_{TR} = \frac{V_Y}{\cos\alpha} \tag{33}$$

Substituting Equation (5b) into Equation (33):

$$V_{TR} = \frac{V_R\left[\frac{b_2}{b_1} + \frac{\alpha_m}{\alpha_1}\left(1 - \frac{b_2}{b_1}\right)\right]\left(\frac{h_2}{R} + \alpha_m^2\right)\cos\alpha_m}{\left[\frac{b_2}{b_1} + \frac{\alpha}{\alpha_1}\left(1 - \frac{b_2}{b_1}\right)\right]\left(\frac{h_2}{R} + \alpha^2\right)\cos\alpha} \tag{34}$$

The velocity of the roll surface in the X direction is zero, and in the tangential direction is V_R. The resultant velocity discontinuity thus becomes:

$$\Delta V_3^2 = (V_X - 0)^2 + (V_{TR} - V_R)^2 \tag{35}$$

Simplifying:

$$\Delta V_3 = \sqrt{V_X^2 + V_{TR}^2 - 2\,V_{TR}V_R + V_R^2} \tag{36a}$$

Combining Equations (32), (34), and (36a) yields the required velocity discontinuity on surface S_3:

$$\Delta V_3 = V_R \sqrt{\frac{\left[\frac{b_2}{b_1} + \frac{\alpha_m}{\alpha_1}\left(1 - \frac{b_2}{b_1}\right)\right]^2\left(\frac{h_2}{R} + \alpha_m^2\right)^2\cos^2\alpha_m}{\left[\frac{b_2}{b_1} + \frac{\alpha}{\alpha_1}\left(1 - \frac{b_2}{b_1}\right)\right]^2\left(\frac{h_2}{R} + \alpha^2\right)^2\cos^2\alpha}} \cdot$$

$$\sqrt{\left\{\frac{\left(\frac{b_2}{b_1} - 1\right)^2 X^2}{R^2\alpha_1^2\left[\frac{b_2}{b_1} + \frac{\alpha}{\alpha_1}\left(1 - \frac{b_2}{b_1}\right)\right]^2} + 1\right\}} \quad -$$

$$\left.\frac{2\left[\frac{b_2}{b_1}+\frac{\alpha_M}{\alpha_1}\left(1-\frac{b_2}{b_1}\right)\right]\left(\frac{h_2}{R}+\alpha_m^2\right)\cos\alpha_m}{\left[\frac{b_2}{b_1}+\frac{\alpha}{\alpha_1}\left(1-\frac{b_2}{b_1}\right)\right]\left(\frac{h_2}{R}+\alpha^2\right)\cos\alpha}+1\right] \tag{36b}$$

The friction loss power is evaluated through Equation (31) by integrating Equation (36b) with respect to X and α. The X integration can be handled with integral tables, but the α integration is hopelessly complicated. For this reason, an approximation was made for $\dot{W}_F$. In Figure 5, the arc of contact between roll and workpiece is projected onto the X-Y plane. Line M-N divides the contact area in half. Equation (31) can be approximated by:

$$\dot{W}_F \cong \frac{4m\sigma_o}{\sqrt{3}}\left[(\Delta V_{3A})(S_{3A})+(\Delta V_{3B})(S_{3B})\right] \tag{37}$$

ΔV_{3A} is the resultant velocity discontinuity at Point A and S_{3A} is the surface area over which ΔV_{3A} is assumed to be constant. Similarly, ΔV_{3B} is the resultant velocity discontinuity at Point B and S_{3B} is the surface area over which ΔV_{3B} is assumed to be constant. Since the velocity discontinuity actually changes from point to point throughout surface S_3, a greater number of terms in the approximation (i.e., smaller subdivisions of surface S_3) results in better accuracy. The two-term approximation used above was compared with four and eight-term approximations. The four-term approximation was within

2% of the eight-term approximation, and the two-term approximation was within 3% of the eight-term approximation.

Using Equation (36b) to evaluate ΔV_{3A} and ΔV_{3B}, $\dot{W}_F$ is, by Equation (37):

$$\frac{\dot{W}_F}{\frac{\sigma_0 V_R R^2}{\sqrt{3}}} = \frac{n}{4}\sqrt{\frac{h_2}{R}\left(\frac{h_1}{h_2}-1\right)}\left(\frac{b_1}{R}\right)\left(\frac{b_2}{b_1}+3\right) \cdot$$

$$\sqrt{\frac{16\left[\frac{b_2}{b_1}+\frac{\alpha_m}{\alpha_1}\left(1-\frac{b_2}{b_1}\right)\right]^2\left(\frac{h_2}{R}+\alpha_m^2\right)^2\cos^2\alpha_m}{\left(\frac{b_2}{b_1}+3\right)^2\left[\frac{h_2}{R}+\frac{9}{16}\left(\frac{h_2}{R}\right)\left(\frac{h_1}{h_2}-1\right)\right]^2\cos^2\left(\frac{3}{4}\sqrt{\frac{h_2}{R}\left(\frac{h_1}{h_2}-1\right)}\right)}} \cdot$$

$$\left[\frac{\left(\frac{b_2}{b_1}-1\right)^2\left(\frac{b_1}{R}\right)^2}{16\left(\frac{h_2}{R}\right)\left(\frac{h_1}{h_2}-1\right)}+1\right] -$$

$$\sqrt{\frac{8\left[\frac{b_2}{b_1}+\frac{\alpha_m}{\alpha_1}\left(1-\frac{b_2}{b_1}\right)\right]\left(\frac{h_2}{R}+\alpha_m^2\right)\cos\alpha_m}{\left(\frac{b_2}{b_1}+3\right)\left[\frac{h_2}{R}+\frac{9}{16}\left(\frac{h_2}{R}\right)\left(\frac{h_1}{h_2}-1\right)\right]\cos\left(\frac{3}{4}\sqrt{\frac{h_2}{R}\left(\frac{h_1}{h_2}-1\right)}\right)}+1} +$$

$$\frac{m}{4}\sqrt{\frac{h_2}{R}\left(\frac{h_1}{h_2}-1\right)}\left(\frac{b_1}{R}\right)\left(3\,\frac{b_2}{b_1}+1\right)\cdot$$

$$\sqrt{\frac{16\left[\frac{b_2}{b_1}+\frac{\alpha_M}{\alpha_1}\left(1-\frac{b_2}{b_1}\right)\right]^2\left(\frac{h_2}{R}+\alpha_M^2\right)^2\cos^2\alpha_M}{\left(3\,\frac{b_2}{b_1}+1\right)^2\left[\frac{h_2}{R}+\frac{1}{16}\left(\frac{h_2}{R}\right)\left(\frac{h_1}{h_2}-1\right)\right]^2\cos^2\left(\frac{1}{4}\sqrt{\frac{h_2}{R}\left(\frac{h_1}{h_2}-1\right)}\right)}}\cdot$$

$$\left[\frac{\left(\frac{b_2}{b_1}-1\right)^2\left(\frac{b_1}{R}\right)^2}{16\left(\frac{h_2}{R}\right)\left(\frac{h_1}{h_2}-1\right)}+1\right]-$$

$$\sqrt{\frac{8\left[\frac{b_2}{b_1}+\frac{\alpha_M}{\alpha_1}\left(1-\frac{b_2}{b_1}\right)\right]\left(\frac{h_2}{R}+\alpha_M^2\right)\cos\alpha_M}{\left(3\,\frac{b_2}{b_1}+1\right)\left[\frac{h_2}{R}+\frac{1}{16}\left(\frac{h_2}{R}\right)\left(\frac{h_1}{h_2}-1\right)\right]\cos\left(\frac{1}{4}\sqrt{\frac{h_2}{R}\left(\frac{h_1}{h_2}-1\right)}\right)}}+1 \qquad (38)$$

$\frac{\dot{W}_F}{\frac{\sigma_0 V_R R^2}{\sqrt{3}}}$ is a convenient non-dimensional form of the friction loss power over the roll contact surfaces S_3.

Solution for Spread

The total process power (in the absence of forces on the workpiece external to the roll contact zone and due to inertia) is:

$$\frac{J^*}{\frac{\sigma_0 V_R R^2}{\sqrt{3}}} = \frac{\dot{W}_I + \dot{W}_{S_1} + \dot{W}_{S_2} + \dot{W}_F}{\frac{\sigma_0 V_R R^2}{\sqrt{3}}} \qquad (39)$$

and is a function of 6 variables:

$$\frac{h_1}{h_2}, \frac{h_2}{R}, \frac{b_1}{R}, m, \alpha_n, \frac{b_2}{b_1}$$

For a given rolling situation, the first three are known. The friction coefficient, m, can be established indirectly through separate rolling experiments.[18, 19] The Upper Bound Theorem dictates that α_n and b_2/b_1 will take on values that will minimize the power required to roll the workpiece. To obtain an "exact" solution for the spread, h_2/b_1, Equation (39) must first be minimized with respect to α_n:

$$\frac{\partial}{\partial \alpha_m}\left(\frac{J^*}{\frac{\sigma_0 V_R R^2}{\sqrt{3}}}\right) = 0 \qquad (40)$$

and the resultant expression must then be minimized with respect to spread:

$$\frac{\partial}{\partial\left(\frac{b_2}{b_1}\right)}\left(\text{EQUATION (40)}\right) = 0$$

The shear bulk of Equation (39) makes it impractical to attempt the double minimization. Also, an implicit equation in b_2/b_1 would be all that one could hope for. If $\alpha_n=0$, however, only b_2/b_1 would be left as a variable subject to minimization. Although the assumption of $\alpha_n \approx 0$ is a serious departure from many rolling situations, a solution for spread cannot be achieved within the scope of this work without making it. For these reasons, Equations (13b), (20), (29), (38), and (39) were restricted to the case of $\alpha_n=0$. Equation (39) was computed for typical values of the rolling variables using a digital computer. b_2/b_1 was initially set equal to unity (no spread) and was then assigned increasing values in increments of 0.5 percent (b_2/b_1 = 1.000, 1.005, 1.010, etc.). Equation (39) was found to have a single minimum point with respect to variable b_2/b_1. This value of b_2/b_1 is the spread predicted by the Upper Bound Analysis to occur in the actual rolling process.

The computer program for the solution of Equation (39) appears in Appendix III.

RESULTS

Table I is a portion of the digital computer printout for the minimization of J* with respect to b_2/b_1. The heading gives the values of the rolling variables for this particular calculation. b_2/b_1 was assigned increasing values, starting at 1.000, and the four components of rolling power, $\dot{W}_I$ (Equation (13b)), $\dot{W}_{S_1}$ (Equation (20)), $\dot{W}_{S_2}$ (Equation (29)), and $\dot{W}_F$ (Equation (38)) were evaluated separately and combined to determine the value of J*. Also shown is the quantity $J^*-\dot{W}_F$, which is the rolling power for frictionless conditions.

$\dot{W}_I$ and $\dot{W}_F$ each exhibit a minimum with respect to b_2/b_1, in Table I, while $\dot{W}_{S_1}$ and $\dot{W}_{S_2}$ increase monatonically with increasing b_2/b_1. The analysis predicts that the spread under the rolling conditions shown will be b_2/b_1=1.09, since J*, the total rolling power, is minimum at b_2/b_1=1.09. This minimization process was repeated for various rolling conditions to determine their effect on workpiece spread.

Effect of Workpiece Geometry on Spread

Figure 6 shows the effects of workpiece starting width/height ratio and thickness reduction on spread for conditions m=1.0 and h_1/D= 0.05. Workpiece geometry, b_1/h_1, has a large effect on spread. A

narrow workpiece will spread proportionally more than a wide one. At $b_1/h_1=8$, spread becomes almost negligible. As the width of the workpiece increases with respect to its height for a given reduction, the zone of contact between workpiece and rolls becomes longer in the width direction while remaining unchanged in the length direction. The frictional resistance to plastic flow increases in the width direction while remaining unchanged in the length direction, and spreading is reduced in favor of elongation.

Also shown in Figure 6 is experimental data of Chitkara[20] and Wusatowski.[4] Chitkara's data is for rolling lead at room temperature and Wusatowski's is for rolling steel at various elevated temperatures. While the data shows actual spread to be higher than that predicted through Equation (39), the predicted effects of geometry and reduction are verified.

Effect of Roll Diameter on Spread

Figure 7 shows the effects of workpiece thickness/roll diameter ratio and reduction on spread. For constant workpiece starting thickness, h_1, the effect of varying the roll diameter, D, can be seen for a square bar ($b_1/h_1=1.0$) with sticking friction ($m=1.0$). Small rolls ($h_1/D=0.15$) promote low spread while large rolls ($h_1/D=0.01$) promote high spread. This effect can also be explained by the contact zone length in the width and length directions. With a small roll, the contact zone is short in the length direction. With a large roll, the

contact zone length remains unchanged in the width direction but is longer in the length direction. The resulting additional frictional resistance to flow in the length direction favors more spreading at the expense of elongation.

Experimental data of Sparling,[9] Chitkara,[20] and Wusatowski[4] are also shown in Figure 7. Sparling's data is for rolling steel at 1100 degrees centigrade. As in Figure 6, the predicted spread is low compared to the experimental data, but in general the effects of h_1/D and reduction are predicted correctly. The predicted spread agrees best with Sparling's data.

Effect of Friction on Spread

Figure 8 shows the effects of surface friction between rolls and workpiece and reduction on spread for a square workpiece (b_1/h_1= 1.0) and medium size rolls (h_1/D=0.05). When friction is high ($0.5 \leq m \leq 1.0$) spread is high, and when friction is low ($0.05 \leq m \leq 0.1$) spread is low. The predicted drop in spread for $m < 0.4$ and $h_1/h_2 > 1.3$) is worth further consideration. This behavior has not been checked experimentally. However, it is mathematically predicted by the spread model for the following reasons.

$\dot{W}_I$, the internal power of deformation, can be expressed as the product of the work per unit volume and the volume rate. With $\alpha_n > 0$, as is the usual case in rolling, the volume rate is:

$$\dot{V} = b_m h_m V_R \cos \alpha_m$$

As thickness reduction increases (for h_1 constant), α_m decreases to maintain equilibrium conditions in the roll contact zone. This causes b_m and $\cos \alpha_m$ to increase, and h_m to decrease. The volume rate may increase or decrease slightly as a result. With $\alpha_m = 0$, as assumed in the Power Analysis, the volume rate is:

$$\dot{V} = b_2 h_2 V_R$$

As thickness reduction increases (for h_1 constant), $\alpha_m = 0$ must hold, and h_2 decreases. Even if b_2 increases, the decrease in h_2 will be greater and $\dot{V}$ will decrease significantly. This decrease in $\dot{V}$ affects the minimization of $\dot{W}_I$ and causes it to reach its minimum value at a lower value of b_2/b_1 than would otherwise be the case. When friction is high ($0.5 \leq m \leq 1.0$), the behavior of $\dot{W}_I$ does not have a large effect on J*, but when friction is lower ($m < 0.4$), $\dot{W}_I$ is a large part of J* and a decrease in spread with increasing reduction is predicted.

There is no experimental data presently available on the effect of friction coefficient on spread to verify this behavior.

Effect of Reduction on Spread

Figures 6, 7, and 8 all show that spread increases with increasing thickness reduction, except when friction is low. Once again this is explained by considering the length of the contact zone between rolls and workpiece. As reduction increases for constant entry thickness, h_1, the contact zone in the length direction increases in length

and presents greater frictional resistance to elongation of the workpiece. The workpiece finds it easier to deform in the width direction and spread is increased at the expense of elongation.

Comparison With Experimental Data

Figure 9 is a plot of spread predicted by the Upper Bound Power Analysis, Equation (39), vs. actual spread measured experimentally by Chitkara during the rolling of lead at room temperature. Rough rolls (58-64 μ -in. C.L.A.) were used in the experiments. Predicted values of spread are consistently lower than actual values with the disagreement reaching 45% at higher thickness reductions. Friction shear factor m was taken as unity in the Power Analysis. It is also observed that the power analysis underestimates the effect on the spread of using larger rolls.

Figure 10 is a plot of spread predicted by the Power Analysis vs. actual spread measured experimentally by Sparling during the rolling of steel at 1100 degrees centigrade. Again the predicted spread values are lower than the actual spread, by up to 36% at the higher thickness reductions. Friction shear factor m was taken as unity in the Power Aanalysis.

The Power Analysis predicts that spread will increase with:

1. decreasing width/thickness ratio (b_1/h_1)
2. increasing reduction in thickness (h_1/h_2)
3. decreasing thickness/roll diameter ratio (h_1/D)
4. increasing coefficient of friction (m)

Chitkara's and Sparling's experimental data generally agree with 1, 2, and 3. Sparling found that decreasing the amount of workpiece surface scale and increasing the roll roughness (both of which tend to increase roll/workpiece friction) will increase spread. Chitkara, however, noticed that increasing the roll roughness increased the workpiece spread monatonically only for square ($b_1/h_1=1$) workpieces. For other workpiece geometries, he found that increasing friction at first decreased spread, then increased it.

Discussion and Recommendations for Future Work

The assumption that workpiece sides remain straight and parallel throughout the rolling process is a serious departure from the actual case. A few experiments conducted by the author have shown that bulging of the sides can be considerable, especially at higher reductions. The bulging not only increases the apparent spread for a given set of rolling conditions, but more seriously, it alters the mode of deformation from that which would occur if the sides remained straight and parallel. The velocity field chosen for this analysis is, therefore, not the one that exists in actual rolling. Specifically, V_x, the velocity in the width direction, is not independent of Z, the thickness coordinate. A degree of bulging should be postulated to improve the velocity field and agreement with experimental data.

Another departure from actual rolling conditions is the assumption of $\alpha_m = 0$. This assumption is good in some cases, where α_m is actually small in value, but in other cases this assumption distorts

the assumed velocity field seriously compared to the actual one. α_m=0 was assumed to avoid double minimization of J*, first with respect to α_m, then with respect to b_2/b_1. Taking $\alpha_m > 0$ would put the analysis outside the scope of this work, but it should result in better agreement between predicted and observed spread.

Finally, strain hardening should be included in future work. It is unclear what effect strain hardening has on spread; however, strain hardening is proportional to strain, and rolling strain in the width direction is normally less than in the length direction. In actual rolling the workpiece may spread more than would be expected because it is weaker in the width direction than in the length direction as a result of strain hardening.

The author strongly feels that continuation of this work without these simplifying assumptions will improve the spread model to the point where accurate predictions of spread can be made. Then, for the first time, there will be a rational equation for spread available to rolling mill operators and roll designers. Although it will be restricted to the relatively simple (but practically important) case of flat rolling, extension of the analysis to shaped-pass rolling is entirely conceivable. This would be very valuable to roll designers, who at present rely mostly on past experience and trial-and-error techniques to establish pass schedules and roll designs.

CONCLUSIONS

Upper Bound Analysis has been applied to the problem of spread in flat rolling and has yielded a rational mathematical model relating spread to rolling variables such as reduction, roll size, workpiece geometry, and friction. Compared with published experimental data, the predictions of the spread model are generally low. The model correctly predicts, however, that rolling variables have the following effects on spread:

1. increasing reduction increases spread
2. increasing roll diameter increases spread
3. decreasing the workpiece width/thickness ratio increases spread
4. increasing friction increases spread

The first three can be summarized by saying that any change in rolling conditions which decreases the ratio of contact zone lengths in the width and length directions, b/L, will tend to increase spread.

The assumptions of no bulging of workpiece sides, $\alpha_m = 0$, and no strain hardening have resulted in a velocity field different than the actual case in rolling, and this has affected the accuracy of the spread model. A refined analysis that allows for bulging, $\alpha_m > 0$, and strain hardening will bring predicted spread into better

agreement with experimental data, and will result in a spread model of practical importance to roll designers and rolling mill operators.

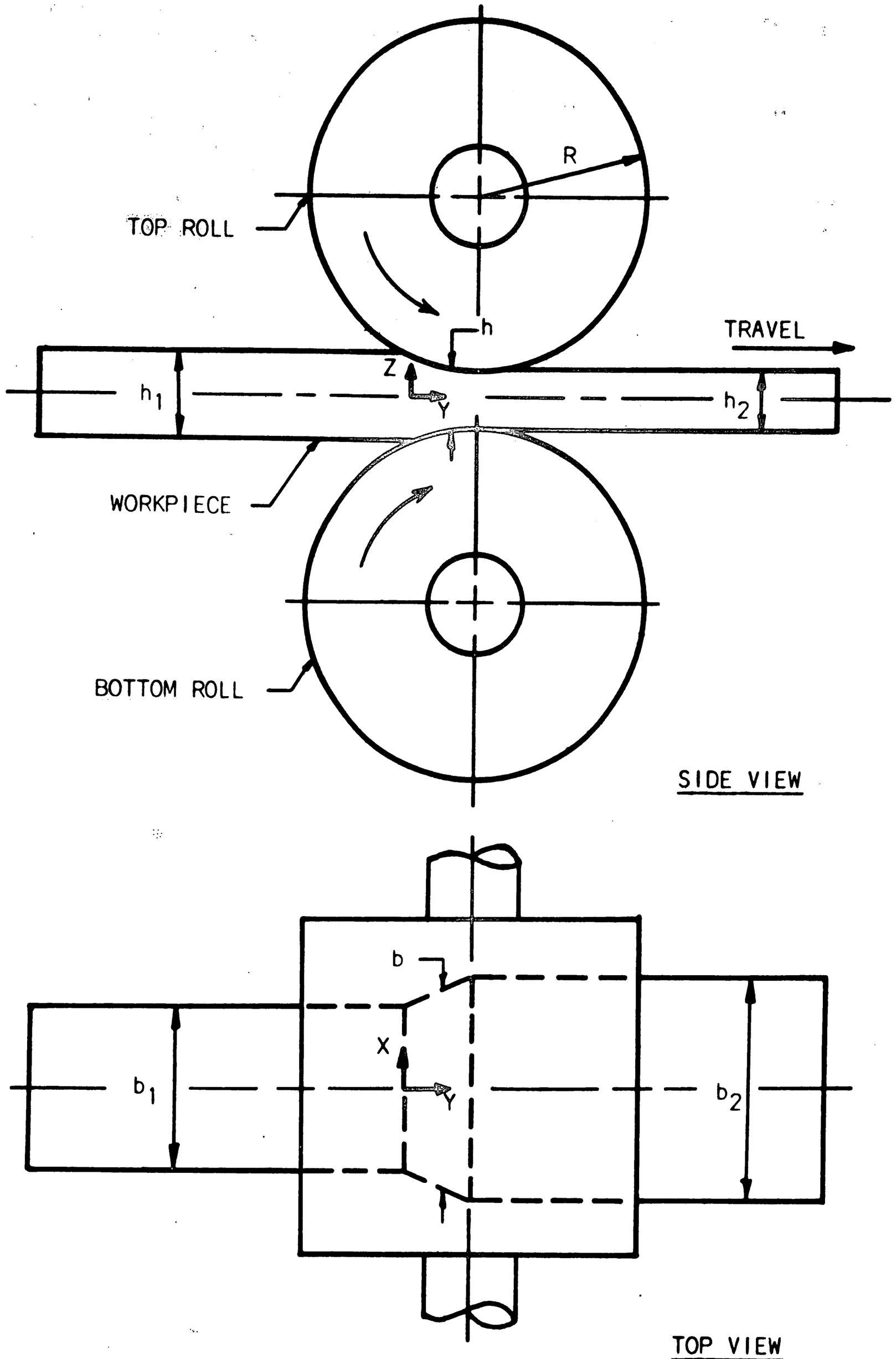

FIGURE 1. THE FLAT ROLLING PROCESS

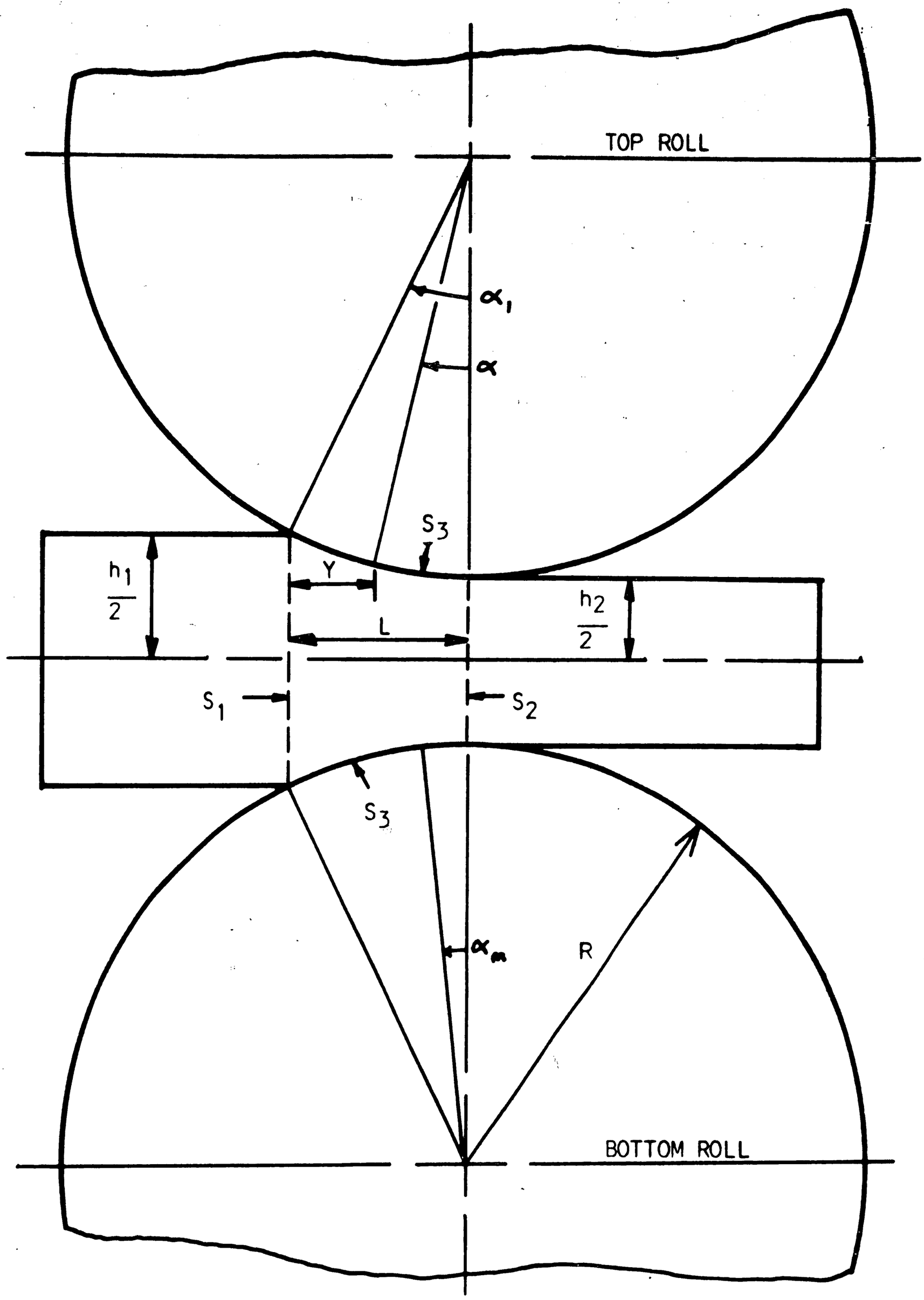

FIGURE 2. ROLL CONTACT ZONE GEOMETRY

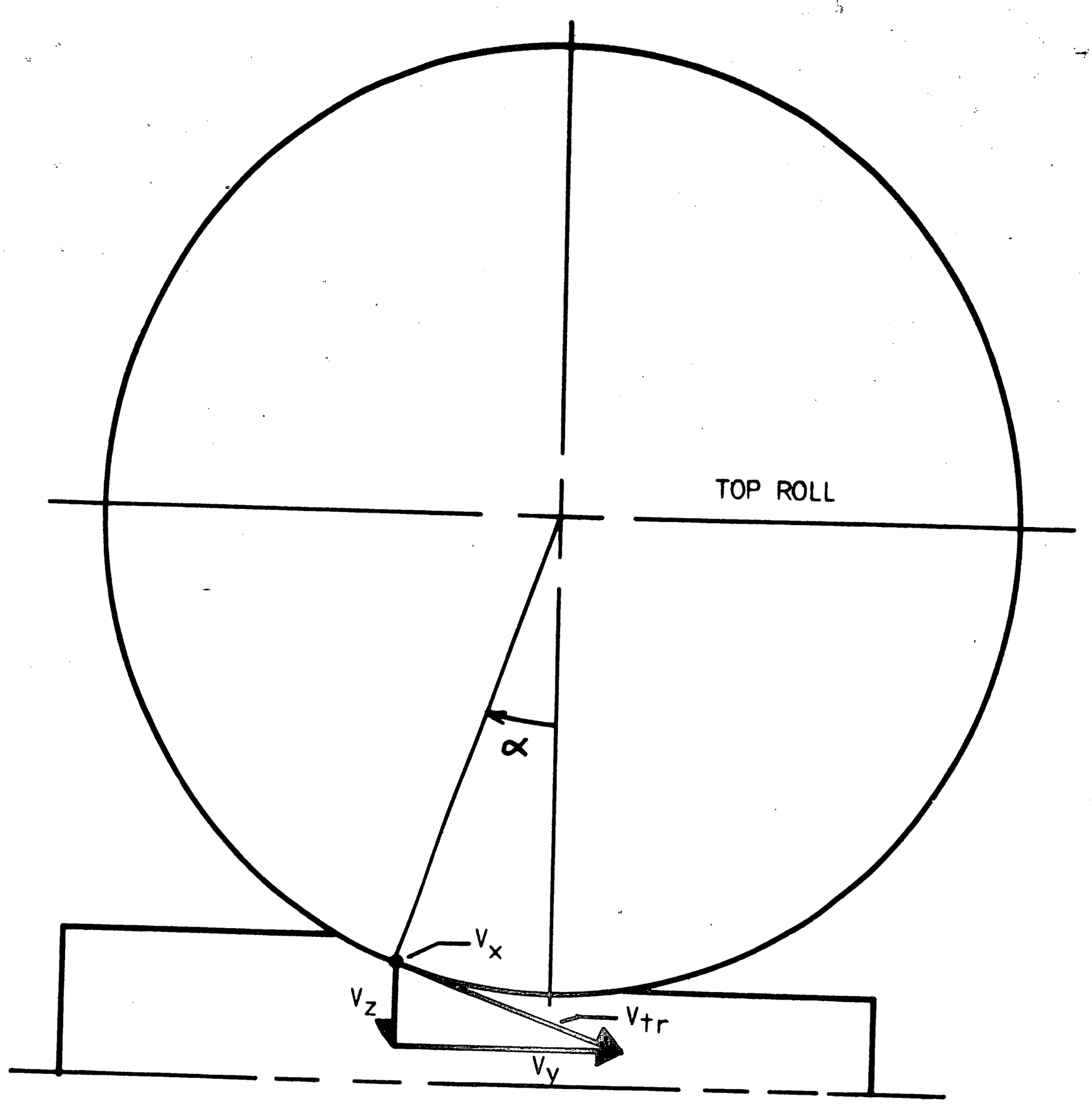

FIGURE 3. RELATIVE VELOCITIES AT ROLL/WORKPIECE CONTACT SURFACES

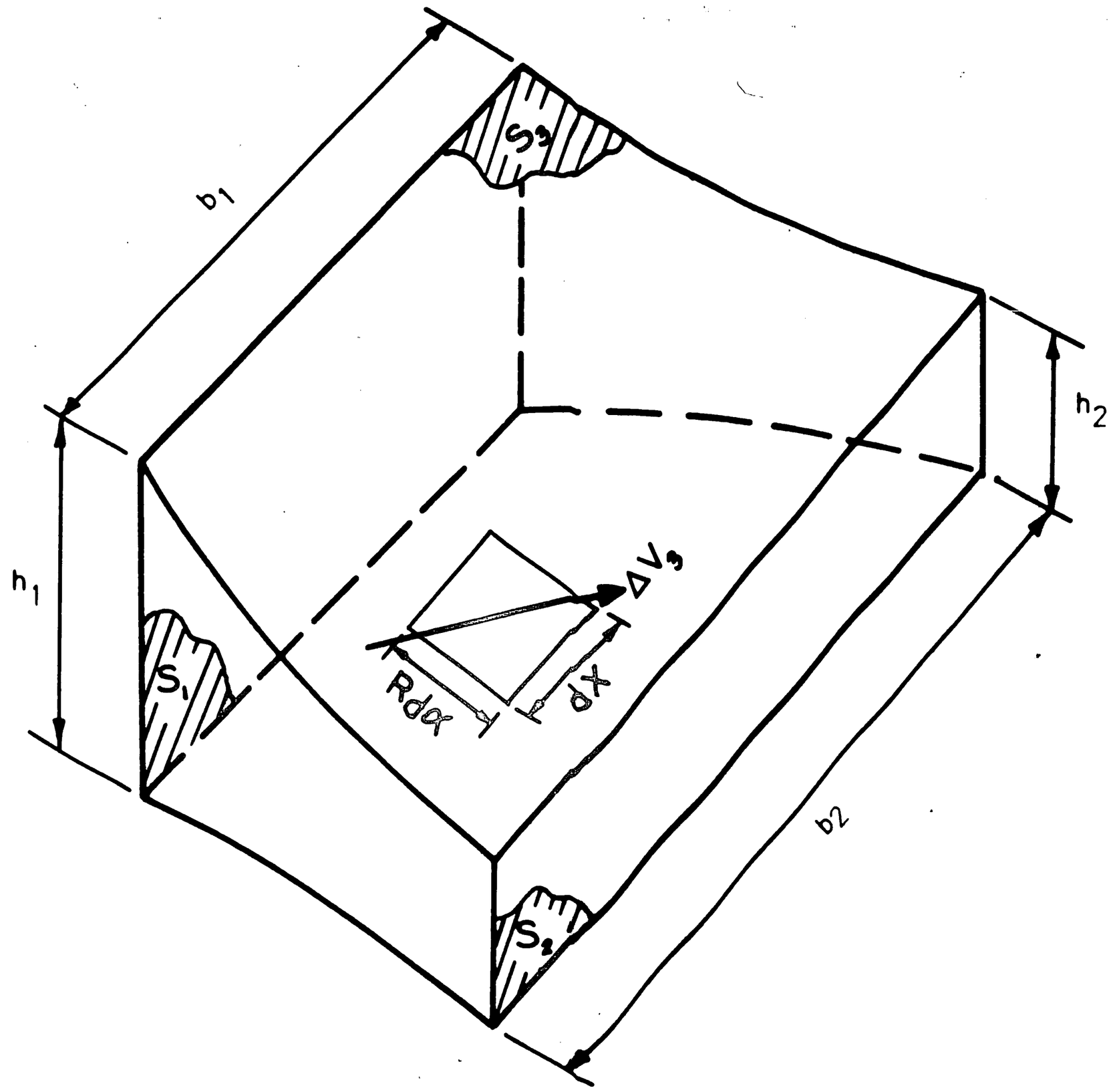

FIGURE 4. PLASTIC DEFORMATION ZONE IN THE WORKPIECE

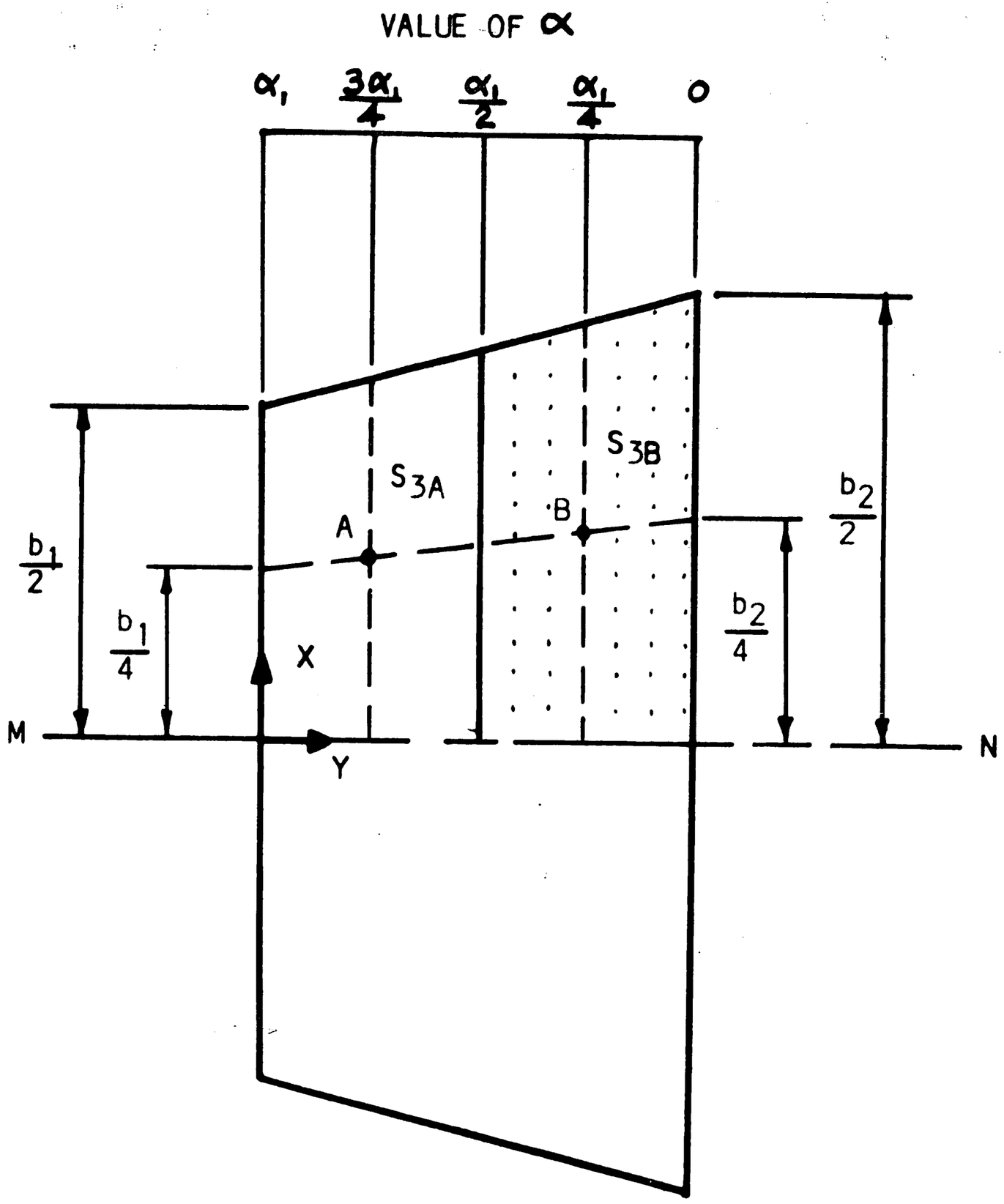

AT POINT A : $\alpha = \frac{3\alpha_1}{4}$, $X = \frac{b_1}{16}\left(\frac{b_2}{b_1} + 3\right)$

AT POINT B : $\alpha = \frac{\alpha_1}{4}$, $X = \frac{b_1}{16}\left(3\frac{b_2}{b_1} + 1\right)$

FIGURE 5. ARC OF CONTACT BETWEEN ROLL AND WORKPIECE PROJECTED ONTO THE X-Y PLANE

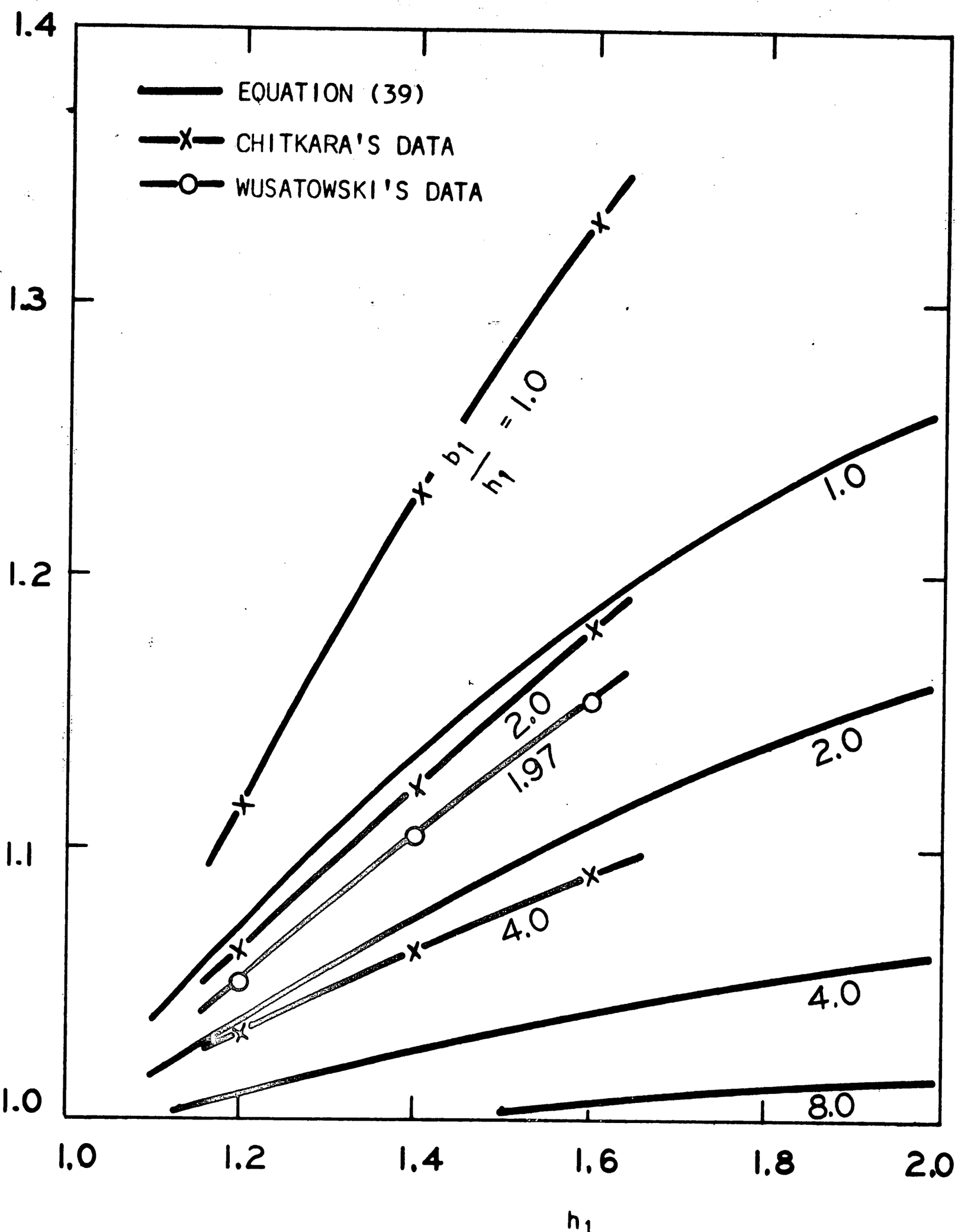

$$\text{REDUCTION} - \frac{h_1}{h_2}$$

$\frac{h_1}{D}$ = 0.05 FOR ALL CURVES, m = 1.0 IN EQUATION (39)

FIGURE 6. THE EFFECTS OF WORKPIECE GEOMETRY AND REDUCTION ON SPREAD

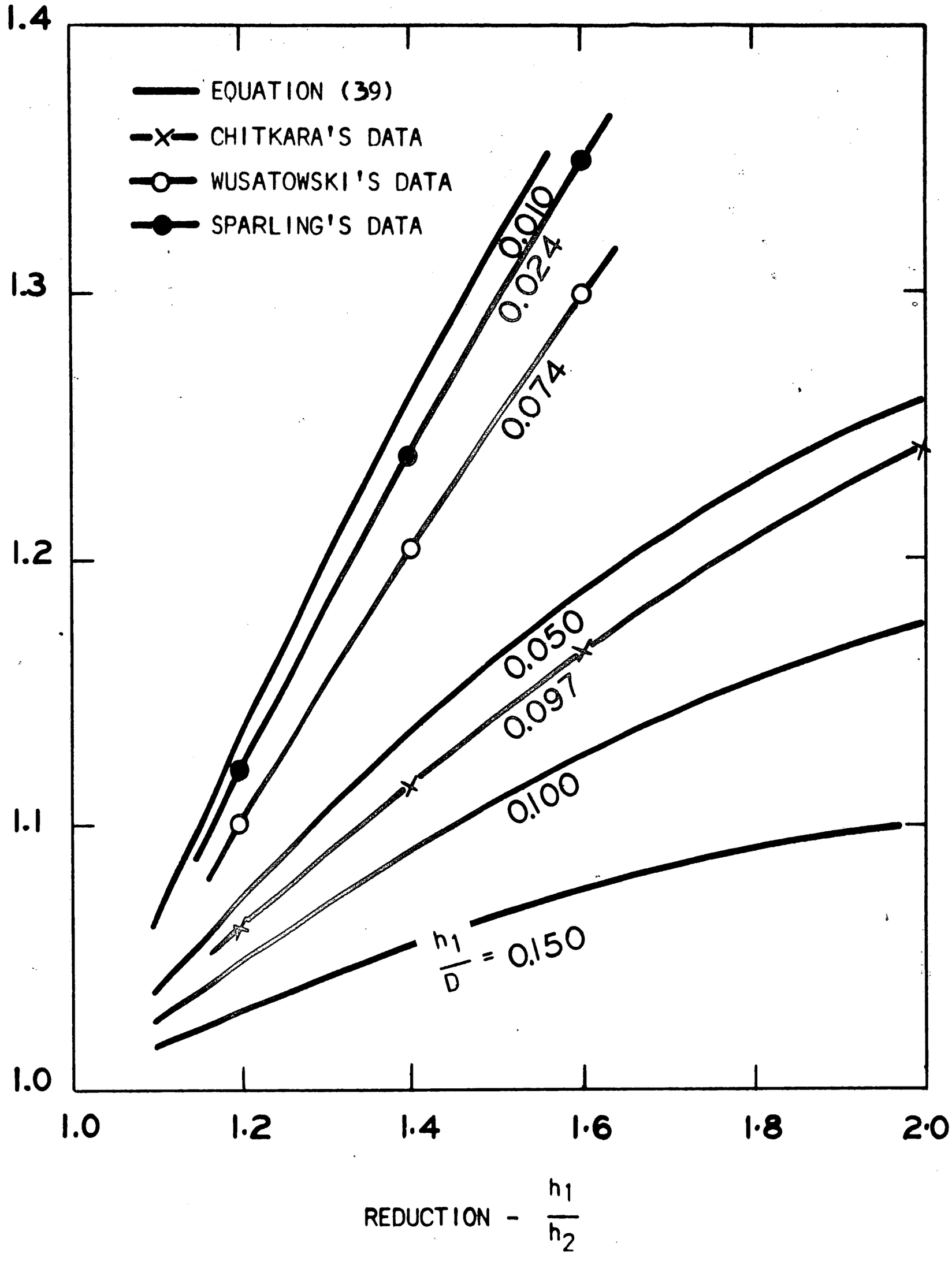

$\frac{b_1}{h_1}$ = 1.0 FOR ALL CURVES, m = 1.0 IN EQUATION (39)

FIGURE 7. THE EFFECTS OF WORKPIECE THICKNESS/ROLL DIAMETER RATIO AND REDUCTION ON SPREAD

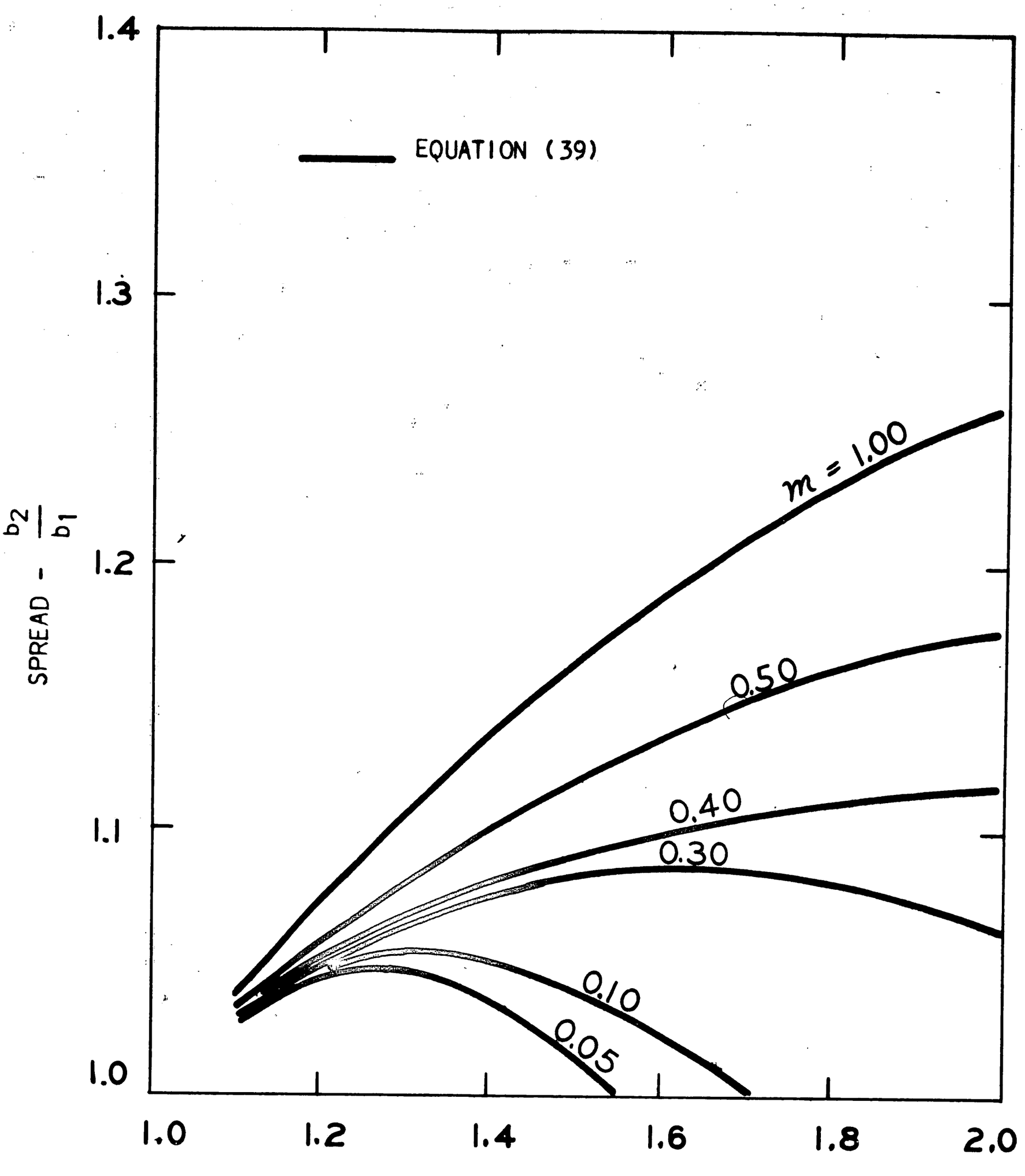

$$\text{REDUCTION} - \frac{h_1}{h_2}$$

$$\frac{h_1}{D} = 0.05, \quad \frac{b_1}{h_1} = 1.0$$

FIGURE 8. THE EFFECTS OF FRICTION SHEAR FACTOR AND REDUCTION ON SPREAD

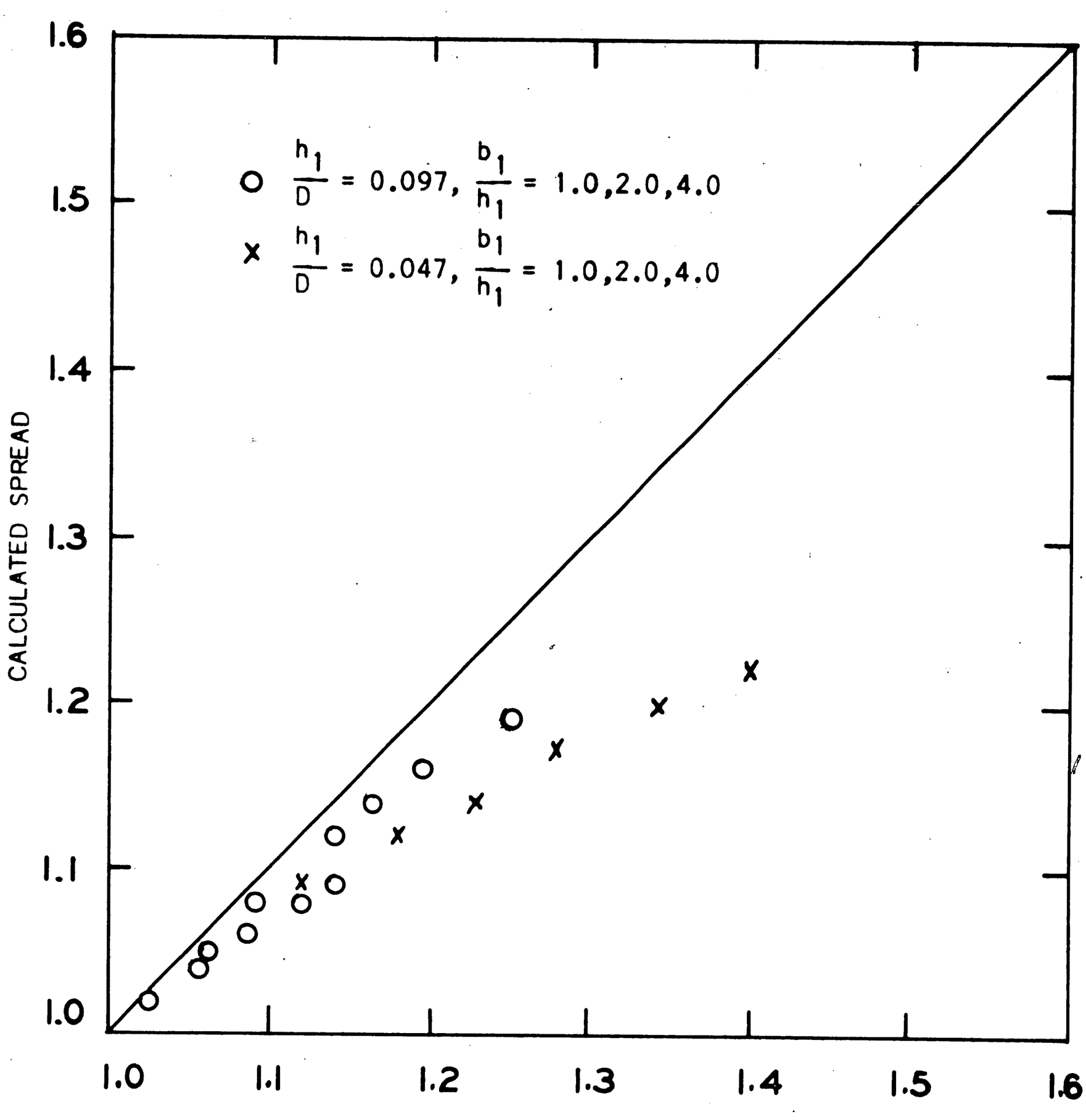

FIGURE 9. COMPARISON OF SPREAD CALCULATED BY EQUATION (39) AND EXPERIMENTAL DATA OF CHITKARA (FOR LEAD ROLLED AT ROOM TEMP.)

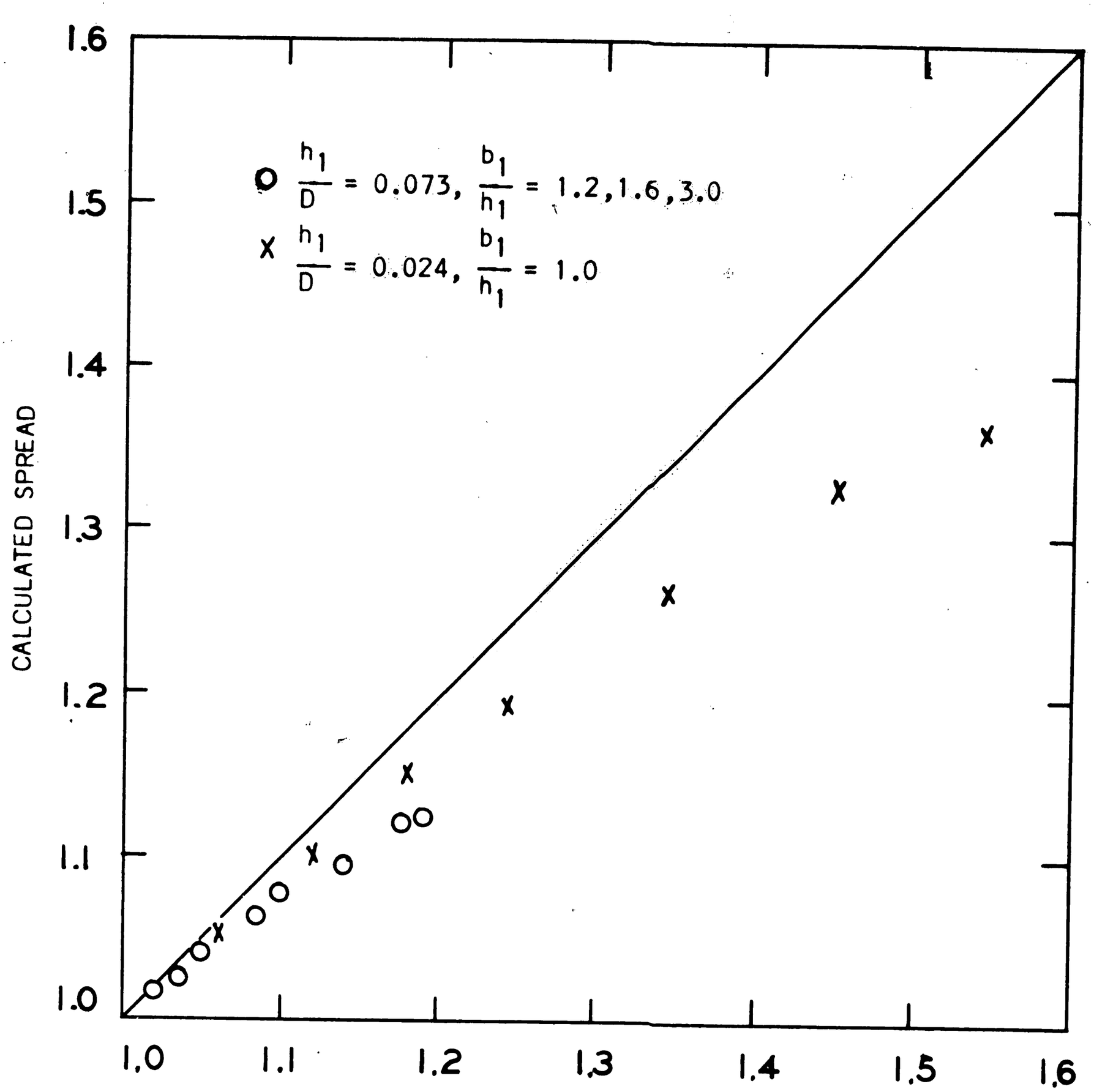

FIGURE 10. COMPARISON OF SPREAD CALCULATED BY EQUATION (39) AND EXPERIMENTAL DATA OF SPARLING (FOR STEEL ROLLED AT 1100 C.)

TABLE 1. TYPICAL COMPUTER PRINTOUT

b_1/R = 0.1000 h_2/R = 0.0800 h_1/h_2 = 1.2500 m = 1.0000 b_1/h_1 = 1.0000 h_1/D = 0.0500

b_2/b_1	$\dot{W}_I$	$\dot{W}_{S1}$	$\dot{W}_{S2}$	$\dot{W}_F$	$J^*-\dot{W}_F$	J^*
1.0000000	0.003570297	0.000569487	0.000000000	0.001882344	0.004139784	0.006022128
1.00500000	0.003548728	0.000572512	0.000007106	0.001821481	0.004128346	0.005949828
1.01000000	0.003528350	0.000575811	0.000014284	0.001761656	0.004118444	0.005880101
1.01500000	0.003509209	0.000579340	0.000021531	0.001703177	0.004110081	0.005813257
1.02000000	0.003491350	0.000583079	0.000028850	0.001646434	0.004103279	0.005749712
1.02500000	0.003474818	0.000587011	0.000036239	0.001591906	0.004098069	0.005689974
1.03000000	0.003459658	0.000591126	0.000043699	0.001540131	0.004094484	0.005634615
1.03500000	0.003445915	0.000595416	0.000051230	0.001491632	0.004092560	0.005584192
1.04000000	0.003433629	0.000599871	0.000058831	0.001446798	0.004092332	0.005539130
1.04500000	0.003422844	0.000604488	0.000066503	0.001405770	0.004093835	0.005499605
1.05000000	0.003413598	0.000609260	0.000074246	0.001368396	0.004097104	0.005465500
1.05500000	0.003405930	0.000614183	0.000082060	0.001334305	0.004102173	0.005436477
1.06000000	0.003399876	0.000619253	0.000089944	0.001303024	0.004109073	0.005412097
1.06500000	0.003395472	0.000624466	0.000097899	0.001274094	0.004117836	0.005391930
1.07000000	0.003392748	0.000629818	0.000105925	0.001247123	0.004128491	0.005375614
1.07500000	0.003391735	0.000635308	0.000114021	0.001221811	0.004141064	0.005362875
1.08000000	0.003392460	0.000640932	0.000122188	0.001197941	0.004155580	0.005353521
1.08500000	0.003394947	0.000646687	0.000130426	0.001175371	0.004172060	0.005347431
1.09000000	0.003399219	0.000652572	0.000138734	0.001154015	0.004190525	0.005344540
1.09500000	0.003405293	0.000658584	0.000147114	0.001133842	0.004210991	0.005344832
1.10000000	0.003413185	0.000664722	0.000155563	0.001114859	0.004233470	0.005346330
1.10500000	0.003422909	0.000670982	0.000164084	0.001097116	0.004257975	0.005355091
1.11000000	0.003434473	0.000677364	0.000172675	0.001080697	0.004284513	0.005365210
1.11500000	0.003447885	0.000683866	0.000181338	0.001065722	0.004313089	0.005378811
1.12000000	0.003463147	0.000690486	0.000190070	0.001052354	0.004343704	0.005396058
1.12500000	0.003480260	0.000697223	0.000198874	0.001040793	0.004376357	0.005417150
1.13000000	0.003499221	0.000704076	0.000207748	0.001031284	0.004411045	0.005442329
1.13500000	0.003520025	0.000711042	0.000216693	0.001024119	0.004447760	0.005471880
1.14000000	0.003542663	0.000718122	0.000225708	0.001019636	0.004486494	0.005506129
1.14500000	0.003567125	0.000725313	0.000234795	0.001018212	0.004527233	0.005545445
1.15000000	0.003593397	0.000732614	0.000243952	0.001020257	0.004569962	0.005590219
1.15500000	0.003621462	0.000740025	0.000253180	0.001026188	0.004614666	0.005640854
1.16000000	0.003651303	0.000747544	0.000262478	0.001036402	0.004661325	0.005697727
1.16500000	0.003682900	0.000755170	0.000271847	0.001051240	0.004709918	0.005761158
1.17000000	0.003716231	0.000762903	0.000281287	0.001070941	0.004760421	0.005831362
1.17500000	0.003751272	0.000770741	0.000290798	0.001095613	0.004812810	0.005908424
1.18000000	0.003787998	0.000778683	0.000300379	0.001125219	0.004867060	0.005992279
1.18500000	0.003826382	0.000786729	0.000310031	0.001159576	0.004923142	0.006082719
1.19000000	0.003866397	0.000794878	0.000319754	0.001198388	0.004981029	0.006179418
1.19500000	0.003908015	0.000803129	0.000329547	0.001241279	0.005040691	0.006281970
1.20000000	0.003951205	0.000811481	0.000339411	0.001287831	0.005102098	0.006389929
1.20500000	0.003995938	0.000819934	0.000349346	0.001337625	0.005165218	0.006502843

APPENDIX I

NOMENCLATURE

b	Workpiece width
D	Roll diameter
e	Base of natural logarithms
h	Workpiece thickness
Δh	Change in thickness during rolling
J^*	Power externally supplied to rolling process
L	Length of contact zone in X-Y plane in Y-direction
m	Friction shear factor
R	Roll radius
S	Denotes a surface
t	Time
V	Velocity
$\dot{V}$	Volume rate
w	Work per unit volume
$\dot{W}$	Power
X	Width coordinate
Y	Length coordinate
Z	Thickness coordinate

α	Angular coordinate
ε	True strain
$\dot{\varepsilon}$	True strain rate
σ_o	Workpiece flow stress
τ	Shear stress
1	Subscript denoting entry plane conditions
2	Subscript denoting exit plane conditions
3	Subscript denoting roll/workpiece surface conditions
n	Subscript denoting no-slip plane conditions

APPENDIX II

INTEGRATION TO DETERMINE AN EXPRESSION FOR SHEAR LOSS POWER AT THE ROLL ENTRY PLANE

The equation to be integrated is:

$$\dot{W}_{S_1} = \frac{4\sigma_0 V_R \cos\alpha_m}{R\sqrt{3}} \int_{z=0}^{z=\frac{h_1}{2}} \int_{x=0}^{x=\frac{b_1}{2}} \sqrt{a_1 x^2 + c_1}\, dx\, dz \qquad (19)$$

where:

$$a_1 = \frac{\left(\frac{b_2}{b_1} - 1\right)^2 b_m^2 h_m^2}{\alpha_1^2 b_1^2 h_1^2 \cos^2\alpha_1} > 0$$

$$c_1 = \frac{4R^2 \tan^2\alpha_1 b_m^2 h_m^2}{b_1^2 h_1^4} z^2 > 0$$

Integral No. 112, page 65 of reference 17 is used for the integration with respect to X. Equation (19) becomes:

$$\frac{\dot{W}_{S_1}}{\frac{4\sigma_0 V_R \cos\alpha_m}{R\sqrt{3}}} = \int_{z=0}^{z=\frac{h_1}{2}} \left\{ \sqrt{a_2 + c_2 z^2} + c_3 z^2 \left[\ln\left(\frac{c_4 + \sqrt{c_4^2 + c_5^2 z^2}}{c_5 z} \right) \right] \right\} dz$$

where:

$$a_2 = \frac{\left(\frac{b_2}{D_1}-1\right)^2 b_m^2 h_m^2 b_1^2}{64\,\alpha_1^2 h_1^2 \cos^2\alpha_1}\,, \quad c_2 = \frac{R^2 \tan^2\alpha_1 b_m^2 h_m^2}{4 h_1^4}$$

$$c_3 = \frac{2R^2 \tan^2\alpha_1 \cos\alpha_1 b_m h_m \alpha_1}{\left(\frac{b_2}{D_1}-1\right) b_1 h_1^3}\,, \quad c_4 = \frac{\left(\frac{b_2}{D_1}-1\right) b_m h_m}{2\alpha_1 h_1 \cos\alpha_1}$$

$$c_5 = \frac{2R \tan\alpha_1 b_m h_m}{b_1 h_1^2}\,, \quad c_6 = \frac{c_4}{c_5}$$

Rearranging, and separating into three integrals:

$$\frac{\dot{W}_{S_1}}{\frac{4\sigma_0 V_R \cos\alpha_m}{R\sqrt{3}}} = \int_0^{\frac{h_1}{2}} \sqrt{a_2 + c_2 Z^2}\cdot dz \quad -$$

$$c_3 \int_\infty^{\frac{2}{h_1}} \frac{1}{Z_1^4}\left(\ln c_6 Z_1\right) dZ_1 \quad +$$

$$c_3 \int_0^{\frac{h_1}{2}} Z^2 \left[\ln\left(1+\sqrt{1+\frac{Z^2}{c_6^2}}\right)\right] dz$$

where: $Z_1 = 1/Z$

The first term is integrated with integral No. 112, reference 17, and becomes:

$$\frac{h_1}{4}\sqrt{a_2 + \frac{h_1^2}{4}c_2} + \frac{a_2}{2\sqrt{c_2}}\left[\ln\left(\frac{\frac{h_1}{2}\sqrt{c_2} + \sqrt{a_2 + \frac{h_1^2}{4}c_2}}{\sqrt{a_2}}\right)\right]$$

The second term is integrated with integral No. 330, ($m = -4$, $a = c_6$) reference 17, and becomes:

$$\left.\frac{3c_3 \ln(c_6 Z_1) + c_3}{9Z_1^3}\right|_{\infty}^{\frac{2}{h_1}}$$

This expression is indeterminate at the lower limit, and it is evaluated with l'Hôpital's Rule:

$$\lim_{Z_1 \to \infty}\left[\frac{3c_3 \ln(c_6 Z_1) + c_3}{9Z_1^3}\right] = \lim_{Z_1 \to \infty}\left[\frac{\frac{3c_3 c_6}{c_6 Z_1}}{27 Z_1^2}\right]$$

$$= \lim_{Z_1 \to \infty}\left[\frac{c_3}{9Z_1^3}\right]$$

$$= 0$$

The second term then becomes:

$$\frac{c_3 h_1^3 \left[3 \ln\left(\frac{2c_6}{h_1}\right) + 1\right]}{72}$$

The third term is integrated in parts:

$$c_3 \int_0^{\frac{h_1}{2}} z^2 \left[\ln\left(1+\sqrt{1+\frac{z^2}{c_6^2}}\right)\right] dz = \frac{c_3 h_1^3}{24} \ln\left(1+\sqrt{1+\frac{h_1^2}{4c_6^2}}\right) +$$

$$\frac{c_3}{3} \int_0^{\frac{h_1}{2}} \frac{z^2\left(1-\sqrt{1+\frac{z^2}{c_6^2}}\right) dz}{\sqrt{1+\frac{z^2}{c_6^2}}}$$

The latter term is separated into two integrals, one of which is integrated directly, the other of which is integrated with Integral No. 120, reference 17 (with $a = 1/c_6^2$, $c=1$, $X=Z$ and becomes:

$$\frac{c_3}{3} \int_0^{\frac{h_1}{2}} \frac{z^2\left(1-\sqrt{1+\frac{z^2}{c_6^2}}\right) dz}{\sqrt{1+\frac{z^2}{c_6^2}}} = \frac{c_3}{3}\left\{\frac{h_1 c_6^2}{2}\sqrt{1+\frac{h_1^2}{4c_6^2}} - \right.$$

$$c_6^2\left[\frac{h_1}{4}\sqrt{1+\frac{h_1^2}{4c_6^2}} + \frac{c_6}{2}\ln\left(\frac{h_1}{2c_6} + \right.\right.$$

$$\left.\left.\sqrt{1+\frac{h_1^2}{4c_6^2}}\right)\right] - \left.\frac{h_1^3}{24}\right\}$$

The integration is now completed, and the shear loss at the roll entry plane is:

$$\frac{\dot{W}_{S1}}{\frac{4\sigma_0 V_R \cos\alpha_m}{R\sqrt{3}}} = \frac{h_1}{4}\sqrt{a_2 + \frac{h_1^2}{4}c_2} \quad +$$

$$\frac{a_2}{2\sqrt{c_2}}\left[\ln\left(\frac{\frac{h_1}{2}\sqrt{c_2} + \sqrt{a_2 + \frac{h_1^2}{4}c_2}}{\sqrt{a_2}}\right)\right] \quad +$$

$$\frac{c_3}{3}\left\{\frac{h_1^3}{24}\left[3\ln\left(\frac{2c_6}{h_1}\right) + 1\right] \quad +\right.$$

$$\frac{h_1^3}{8}\ln\left(1 + \sqrt{1 + \frac{h_1^2}{4c_6^2}}\right) + \frac{h_1 c_6^2}{2}\sqrt{1 + \frac{h_1^2}{4c_6^2}} -$$

$$c_6^2\left[\frac{h_1}{4}\sqrt{1 + \frac{h_1^2}{4c_6^2}} + \frac{c_6}{2}\ln\left(\frac{h_1}{2c_6} + \sqrt{1 + \frac{h_1^2}{4c_6^2}}\right)\right] -$$

$$\left.\frac{h_1^3}{24}\right\}$$

Substituting for ∂_2, c_2, c_3, and c_6 from page 54 yields Equation (20) in the text.

APPENDIX III. COMPUTER PROGRAM FOR EVALUATING EQUATION (39)

```
                    DISK OPERATING SYSTEM/360 FORTRAN   360N-FO-451 23

      DOUBLE PRECISION BR(50),BFO(90),HFR(50),HOF(50),XM(50),A2,D2,D3,
     1D4,D5,D6,D8,D9,D11,D12,A1,AP1,AP2,AP4,APT,APT1,D1,D7,D10,D13,
     2P1,P2,P3,P4,PT1,PT,HOD(50),BOHO(50)
      READ(1,500) NJ,NL,NM,NN
  500 FORMAT(6I10)
      READ(1,501) (BFO(J),J=1,NJ)
      READ(1,501) (HOF(L),L=1,NL)
      READ(1,501) (XM(M),M=1,NM)
      READ(1,501) (HOD(N),N=1,NN)
      READ(1,501) (BOHO(N),N=1,NN)
  501 FORMAT(8F10.8)
      K = 1
      I = 1
      DO 502 N=1,NN
      DO 502 M=1,NM
      DO 502 L=1,NL
  900 HFR(K) = 2./HOF(L)*HOD(N)
  901 BR(I) = HFR(K)*HOF(L)*BOHO(N)
      A2=DSQRT(HFR(K)*(HOF(L)-1.))
      D2=DSIN(A2)
      D3=DCOS(A2)
      D4= D2/D3
      D5= HFR(K)+.0625*A2*A2
      D6= .25*A2
      D8= HFR(K)+.5625*A2*A2
      D9= .75*A2
      D11=DCOS(D9)
      D12=DCOS(D6)
      WRITE(3,504) BR(I),HFR(K),HOF(L),XM(M),BOHO(N),HOD(N)
  504 FORMAT(1H1,10X,'BO/R= ',F11.8,3X,'HF/R= ',F11.8,3X,'HO/HF= ',
     1F11.8,3X,'M= ',F11.8,3X,'BO/HO= ',F11.8,3X,'HO/D= ',F11.8)
      WRITE(3,505)
  505 FORMAT(1HO,10X,'BF/BO',12X,'WI',12X,'WS1',12X,'WS2',12X,'WF',12X,
     1'J*-WF',12X,'J*'//)
      AP1= 2.*BR(I)*DLOG(HOF(L))*HFR(K)
      AP2= .5*HFR(K)*BR(I)*D4
      AP4=XM(M)*A2*BR(I)*DSQRT(HFR(K)*HFR(K)/(D8*D8*D11*D11)-2.*HFR(K)/
     1(D8*D11)+1.)+XM(M)*A2*BR(I)*DSQRT(HFR(K)*HFR(K)/(D5*D5*D12*D12)-2.
     2*HFR(K)/(D5*D12)+1.)
      APT= AP1+AP2+AP4
      APT1= AP1+AP2
      WRITE(3,507) AP1,AP2,AP4,APT1,APT
  507 FORMAT(10X,'1.0000000',4X,F12.9,3X,F12.9,4X,'0.000000000',3X,
     1F12.9,3X,F12.9,3X,F12.9)
      DO 502 J=1,NJ
  800 D1= DLOG(HOF(L))/DLOG(BFO(J))
  801 D7= BFO(J)-1.
  802 D10=DSQRT(1.+(4.*A2*A2*D2*D2)/(D7*D7*BR(I)*BR(I)))
  803 D13= D7*D7*BR(I)*BR(I)/(16.*A2*A2)+1.
  804 P1= 2.*BR(I)*DLOG(BFO(J))*HFR(K)*BFO(J)*DSQRT(1.-D1+D1*D1)
  805 P2= BFO(J)*HFR(K)*(BR(I)*BR(I)*D7/(6.*A2*D3)*D10+D7*D7*BR(I)**3/(
     124.*A2*A2*D2*D3)*DLOG(2.*A2*D2/(D7*BR(I))+D10)+A2*D4*D4*D3/(3.*D7
     2)*DLOG(D7*BR(I)/(2.*A2*D2)*(1.+D10)))
  806 P3= D7*BFO(J)*HFR(K)*BR(I)*BR(I)/(4.*A2)
```

APPENDIX III, (CONTINUED)

```
11/19/68                    FORTMAIN
  807 P4= .25*XM(M)*A2*BR(I)*(BFO(J)+3.)*DSQRT(16.*BFO(J)*BFO(J)*HFR(K)*
     1HFR(K)/((BFO(J)+3.)**2*D8*D8*D11*D11)*D13-8.*BFO(J)*HFR(K)/((
     2BFO(J)+3.)*D8*D11)+1.)+.25*XM(M)*A2*BR(I)*(3.*BFO(J)+1.)*DSQRT(
     316.*BFO(J)**2*HFR(K)**2/((3.*BFO(J)+1.)**2*D5*D5*D12*D12)*D13-8.*
     48FO(J)*HFR(K)/((3.*BFO(J)+1.)*D5*D12)+1.)
808   PT1= P1+P2+P3
  809 PT= P1+P2+P3+P4
      WRITE(3,506) BFO(J),P1,P2,P3,P4,PT1,PT
  506 FORMAT(9X,F11.8,3X,F12.9,3X,F12.9,3X,F12.9,3X,F12.9,3X,F12.9,3X,
     1F12.9)
  502 CONTINUE
  999 CALL QUIT
      END
```

NOTATION

$BR = \frac{b_1}{R}$

$BFO = \frac{b_2}{b_1}$

$HFR = \frac{h_2}{R}$

$HOF = \frac{h_1}{h_2}$

$XM = m$

$HOD = \frac{h_1}{D}$

$BOHO = \frac{b_1}{h_1}$

REFERENCES

1. Trinks, W., Roll Pass Design - Volume I, Second Edition, Penton Publishing Co., Cleveland, (1933), Chapter II, p. 87.

2. Trinks, W., "On Spreading in Rolling," Blast Furnace and Steel Plant, September 1936, p. 786.

3. Ibid, p. 785.

4. Wusatowski, Z., "Draught, Spread, and Elongation in the Hot Rolling Process," Prace Badawcze, Glownego Instytutu Metalurgii I Odlewnictwa, Gliwice, 1949.

5. Wusatowski, Z., and Wusatowski, R., "The Effect of Speed, Temperature, and Kind of Rolls on Spread and Elongation in the Hot Rolling Process," Prace Badawcze, Glownego Instytutu Metallurgii I Odlewnictwa: Zeszyt II, Gliwice, 1950.

6. Wusatowski, Z., "Hot Rolling - A Study of Draught, Spread, and Elongation," Iron and Steel, February 1955, pp. 49-54, and March 1955, pp. 89-94.

7. Wusatowski, Z., and Szalajda, Z., "Non-Slip Angle and Forward Slip During Rolling Involving Spread," Iron and Steel, February 1959, pp. 61-67.

8. Wusatowski, Z., and Cieslar, R., "Interdependence Between Spread, Elongation, and Draught in the Cold Rolling Process," Archiwum Hutn., Volume 12, 1967, pp. 299-308. (BISI Trans. No. 6269)

9. Sparling, L., "Formula for Spread in Hot Flat Rolling," Proc. Instn. Mech. Engrs., Volume 175, No. 11, 1961.

10. Ibid, p. 605.

11. Ibid, p. 606.

12. Avitzur, B., Metal Forming: Processes and Analysis, McGraw-Hill, New York, (1968), Chapter 2, p. 23.

13. Prager, W., and Hodge, P., Theory of Perfectly Plastic Solids, Chapman and Hall Ltd., London, 1951.

14. Avitzur, Op.cit., p. 63.

15. Ibid, p. 55.

16. Ibid, p. 63.

17. Burington, R., Handbook of Mathematical Tables and Formulas, Third Edition, Handbook Publishers Inc., Sandusky, (1948).

18. Whitton, P., and Ford, H., "Surface Friction and Lubrication in Cold Strip Rolling," Proc. Instn. Mech. Engrs., Volume 165, 1955, pp. 123-140.

19. Avitzur, B., "Maximum Reduction in Cold Strip Rolling," Proc. Instn. Mech. Engrs., Volume 174, 1960, pp. 865-884.

20. Chitkara, N., and Johnson, W., "Some Experimental Results Concerning Spread in the Rolling of Lead, "Trans. ASME - Journal of Basic Engineering, Paper No. 65 - WA/MET-11.

VITA

Richard D. Way, son of Mr. and Mrs. Sherwood Way, was born in Easton, Pennsylvania on March 14, 1941. He received his primary and secondary education in the Wilson Borough, Pennsylvania, school system. He entered Lafayette College in September, 1959, and received a Bachelor of Science Degree, Cum Laude, in Mechanical Engineering in June, 1963.

The author has been employed in the Research Department of the Bethlehem Steel Corporation since his graduation from Lafayette College. He is married to the former Joanne Kindt and has two daughters.